A RULE-BASED APPROACH TO CLASSIFY HUMAN PROTEINUSING DATA MINING TECHNIQUES

A PROJECT REPORT

Submitted by

Animesh Upadhyaya -
BWU/BTS/19/060

in fulfilment for the award of the degree of

Bachelor of Technology in Computer Science and Engineering

Department of Computer Science and Engineering

BRAINWARE UNIVERSITY

398, Ramkrishnapur Road, Barasat, North 24 Parganas, Kolkata - 700 125
01 July, 2023

A RULE-BASED APPROACH TO CLASSIFY HUMAN PROTEINUSING DATA MINING TECHNIQUES

Submitted by

Animesh Upadhyaya - BWU/BTS/19/060

in partial fulfilment for the award of the degree
of

BACHELOR OF TECHNOLOGY

in

Computer Science and Engineering

BRAINWARE UNIVERSITY

398, Ramkrishnapur Road, Barasat, North 24 Parganas, Kolkata - 700 125

BONAFIDE CERTIFICATE

BRAINWARE UNIVERSITY

398, Ramkrishnapur Road, Barasat, North 24 Parganas, Kolkata - 700 125

[DEPARTMENT OF COMPUTER SCIENCE and ENGINEERING]

BONAFIDE CERTIFICATE

Certified that this project report **"Aerial images-based forest fire detection for firefighting using optical remote sensing techniques and unmanned aerialvehicles.**

" is the
Bonafede work of
"**Animesh Upadhyaya**" who carried out the project work under my supervision.

SIGNATURE

GUIDE SIGNATURE

Mr. Subhra Prokash Dutta

HEAD OF THE DEPARTMENT
BRAINWARE UNIVERSITY

398, Ramkrishnapur
Road, Barasat, North24
parganas

i

Abstract: Forest fires cause major damage to the environment, human health, and property, and endanger life. We propose a platform that uses Unmanned Aerial Vehicles (UAVs), which constantly patrol over potentially threatened fire areas. It is also possible to use security cameras and special-purpose infrared surveillance cameras for fire detection. The proposed algorithm uses RGB and YCbCr color space. The advantage of using YCbCr color space is that it can separate the luminance from the chrominance more effectively than RGB color space. This requires intelligent video processing techniques for the detection and analysis of uncontrolled fire behavior. It is possible to cover an area of 100 km^2 using a single pan-tilt-zoom camera for wildfire detection. Another benefit of the VFD systems is that they can provide crucial information about the size and growth of the fire, and the direction of smoke propagation. The droning system is self-controlled and secured by LoRa protocol, in every second a base station is received the latitude and longitude. We are cross-checking with remote sensing. Fires can be monitored and analyzed over large areas in a timely and cost-effective manner by using satellite sensor imagery in combination with spatial analysis as provided by Geographical Information Systems (GIS). The optical remote sensing technologies are used in early fire warning systems and provide an extensive survey on both flame and smoke detection algorithms employed by each technology. Three types of systems are identified, namely terrestrial, airborne, and spaceborne-based systems, while various models aiming to detect fire occurrences with high accuracy in challenging environments are studied. Finally, the strengths and weaknesses of fire detection systems based on optical remote sensing are discussed aiming to contribute to future research projects for the development of early warning fire systems.

Keywords: Remote Sensing, VFD, LoRa, GIS, Fire Detection, Machine Learning

1. Introduction:

Over the last few years, climate change and human-caused factors have had a significant impact on the environment. Some of these events include heat waves, droughts, dust storms, floods, hurricanes, and wildfires. Wildfires have extreme consequences on local and global ecosystems and cause serious damage to infrastructure, injuries, and losses in human lives; therefore, fire detection and the accurate monitoring of the disturbance type, size, and impact over large areas is becoming increasingly important [1]. To this end, strong efforts have been made to avoid or mitigate such consequences by early fire detection or fire risk mapping [2]. Traditionally, forest fires were mainly detected by human observation from fire lookout towers and involved only primitive tools, such as the Osborne fire Finder [3]; however, this approach is inefficient, as it is prone to human error and fatigue. On the other hand, conventional sensors for the detection of heat, smoke, flame, and gas typically take time for the particles to reach the point of sensors and activate them. In addition, the range of such sensors is relatively small, hence, a large number of sensors need to be installed to cover large areas [4].

Recent advances in computer vision, machine learning, and remote sensing technologies offer new tools for detecting and monitoring forest fires, while the development of new materials and microelectronics have allowed sensors to be more efficient in identifying active forest fires.

ii

Unlike other fire detection review papers that have focused on various sensing technologies [5],on video flame or/and smoke methodologies in visible or/and InfraRed (IR) range [6–9], on various environments [10], and airborne systems [11,12], in this paper, we provide a comprehensive study of the most representative forest fire detection systems, focusing on thosethat use optical remote sensing, as well as digital image processing [13] and classification techniques [14]. Depending on the acquisition level, three broad categories of widely used systems that can detect or monitor active fire or smoke incidents in real/near-real-time are identified and discussed, namely terrestrial, aerial, and satellite. These systems are usually equipped with visible, IR, or multispectral sensors whose data are processed by machine learningmethods. These methods rely either on the extraction of handcrafted features or on powerful deep learning networks (Figure 1) for early detection of forest fires (Figure 2) as well as for modeling fire or smoke behavior. Finally, we present the strengths and weaknesses of the aforementioned methods and sensors, as well as future trends in the field of early fire detection.

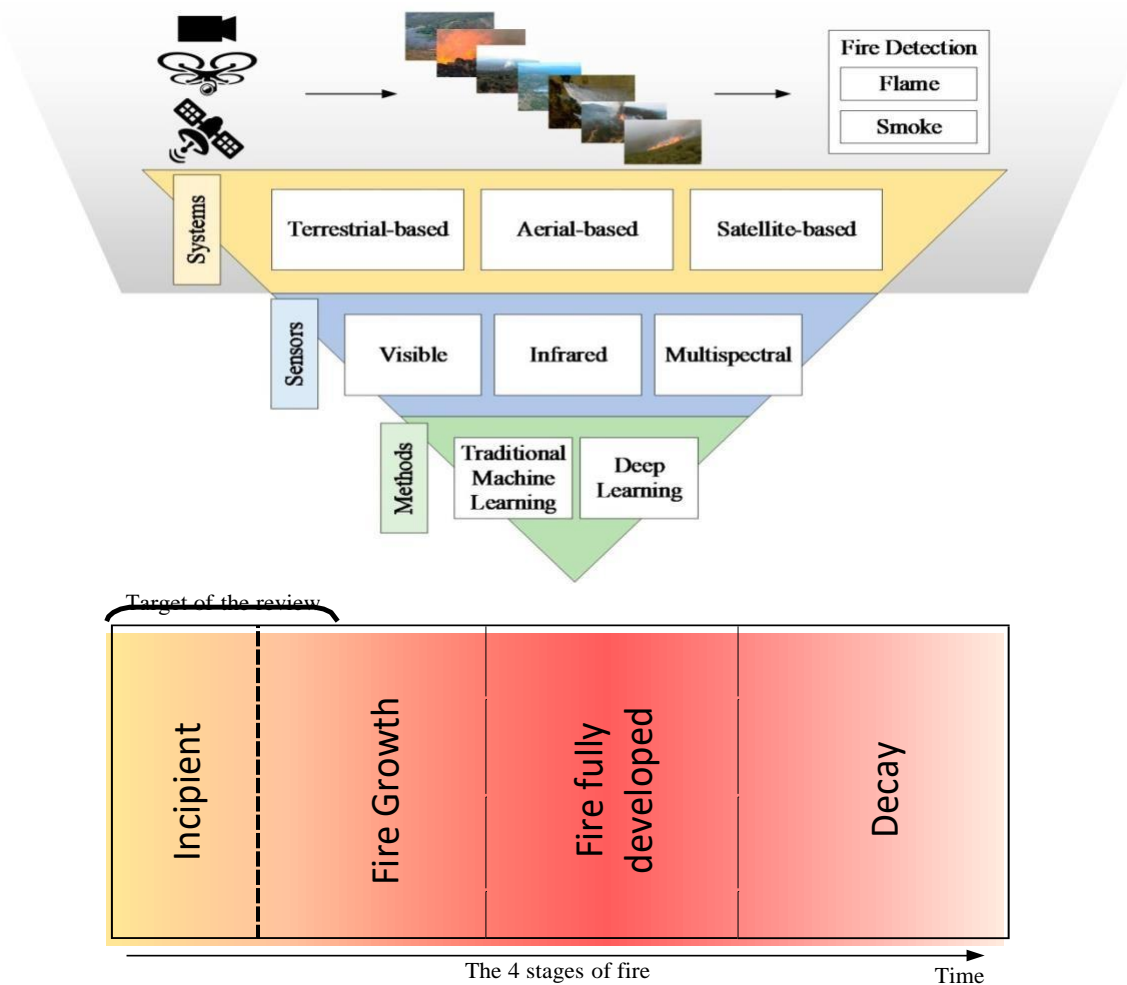**Figure 1.** Generalized multispectral imaging systems for early fire detection.

Figure 2. Systems discussed in this review target the detection of fire in the early stages of the fire cycle.

2. Early Fire Detection Systems

2.1. Terrestrial Systems

Terrestrial-based early detection systems consist of either individual sensors (fixed, PTZ, or 360◦ cameras) or networks of ground sensors. These sensors need to be carefully placed to ensure adequate visibility. Thus, they are usually located in watchtowers, which are structures located on high vantage points for monitoring high-risk situations and can be used not only for detection but also for verification and localization of reported fires. There are two types of cameras used for early fire detection, namely optical cameras and IR cameras that can capture data ranging from low resolution to ultra-high resolution for different fire detection scenarios [15]. Optical cameras provide color information, whereas IR imaging sensors can provide a measure of the thermal radiation emitted by objects in the scene [16]. More recently, early detection systems that combine both types have also been introduced. The computer-based methods can process a high number of data aiming to achieve a consistent level of accuracy maintaining a low false alarm rate. In the following, we first present traditional approaches that are based on handcrafted features followed by more recent methods using deep learning for automated feature extraction.

2.1.1. Traditional Methods

Detection methods that use optical sensors or RGB cameras combine features that are related to the physical properties of flame and smoke, such as color, motion, spectral, spatial, temporal, and texture characteristics. The following color spaces have been used for the task of early fire detection: RGB [17–19], YCbCr [20], CIELAB [21], YUV [22,23], and HSV [24]; however, a drawback of color-based fire detection models is the high false alarm rates, since single-color information is insufficient in most cases for the early and robust fire detection. Thus, many of the developed methodologies combine color and motion information in images and videos [25]. Zhang et al.
[26] used a probabilistic color-based model for the detection of fire regions and motion features for the final fire existence occurrence decision. Avgerinakis et al. [27] identified the smoke candidate blocks and then constructed the histograms of oriented gradients (HOGs) and histograms of optical flow (HOFs), thus considering both appearance and motion information. Likewise, Mueller et al. [28] used two optical flow schemes, namely optimal mass transport models and data-driven optical flow models.

Other researchers focused on the flickering effect of fire. This is observed in flame contours at a frequency of around 10 Hz, independently of the burning material and the burner [29]. To this end, Gunay et al. [30] distinguished flame flicker from the motion of fire-colored moving objects in videos using hidden Markov models (HMMs). Training HMMs leads to the reduction of data redundancy and improvement of reliability, while real-time detection is also achieved [31]. Furthermore, HMM-based methods for fire detection in the compressed domain have been proposed in MJPEG2000 [32] and

H. 264 [33] compressed video. The use of multi-feature fire-based detection can offer more accurate results. Chen et al. [34] combined motion detection using a Gaussian mixture model, color analysis using an RGB color filtering, and flickering temporal analysis. The algorithm was applied to a video dataset consisting of different daytime and nighttime environments; however, at night, color analysis is less useful and night smoke is less visible. Thus, nighttime wildfire detection typically relies on motion analysis. Also, Töreyin, et al. [35] proposed a system equipped with an optical camera and a methodology that combines feature extraction (moving pixel/region extraction, color-based segmentation, and wavelet analysis in temporal and spatial domains), followed by a voting-based classifier. In [36], Barmpoutis et al. extracted an additional feature aiming to estimate a spatio–temporal consistency energy. Thereafter, they used a support vector machine (SVM) classifier to increase the robustness of fire detection.

Many other researchers have used infrared cameras aiming to reduce the false alarm rates of the optical-based terrestrial systems. The IR cameras measure the thermal radiation emitted by objects within the spectral range from either 3 to 5 µm (middle wavelength infrared, MWIR) or 8 to 14 µm (long wavelength infrared, LWIR). The MWIR band detectors, although they are optimal for fire detection, are expensive due to the cooling system required, so typically LWIR cameras are used. In IR videos the existence of rapid time-varying contours is an important sign of the presence of fire in the scene. Arrue et al. [37] observed that fire detection systems fail for distant fires and proposed a system for false alarm reduction in infrared forest-fire detection. More specifically, they used an adaptive infrared threshold, a segmentation method, and a neural network for early fire detection. Furthermore, Töreyin, et al. [16] used IR video to overcome the limitations of optical cameras in the detection of fires with little radiance in the visible spectrum. Specifically, they first estimated the boundaries of moving bright regions in each frame and then used spatio–temporal analysis in the wavelet domain using HMMs.

In contrast to single-sensor systems, multisensor systems typically cover wider areas and can achieve higher accuracies by fusing data from different sensors. The idea of integrated early fire detection and monitoring by combining data from optical and infrared cameras as well as a wireless sensor network (WSN) of temperature/humidity sensors was proposed by Grammalidis et al. [38]. Sensor data were processed and transmitted to a monitoring center employing computer vision and pattern recognition algorithms for automated fire detection and localization. The algorithm took into account color, spatial, and temporal information for flame detection, while for smoke detection, an online adaptive decision fusion (ADF) framework was developed. This framework consisted of several algorithms aiming to detect slow-moving objects, smoke-colored regions, and smoke region smoothness. Furthermore, improved early wildfire detection was achieved by fusing smoke detection from visual cameras and flame detection from infrared (LWIR) cameras. Similarly, Bosch et al. [39] proposed a system consisting of a wireless sensor network with a central monitoring station. In this, each sensor consists of an optical and a thermal camera and an integrated system for the processing of data and communication.

More recently, Barmpoutis et al. [40] and Dimitropoulos et al. [41] introduced fire detection systems based on smoke and flame dynamic texture analysis through linear dynamical systems (LDSs). Their modeling, combining color, motion, and spatio–temporal features led to higher detection rates and a significant reduction of false alarms. Temporal and spatial dynamic texture

v

analysis of flame for forest fire detection was performed in [42]. Dynamic texture features were derived using two-dimensional (2D) spatial wavelet decomposition in the temporal domain and three-dimensional (3D) volumetric wavelet decomposition. In [43], the authors improved the smoke modeling of the fire incidents through dynamic textures solving higher order LDS (h-LDS). Finally, in [44], the authors took the advantage of the geometric properties of stabilized h-LDS (sh-LDS) space, and they proposed a novel descriptor, namely, histograms of Grassmannian points (HoGP) to improve the classification of both flame and smoke sequences.

2.1.2. *Deep Learning Methods*

In contrast to previously discussed methods that rely on handcrafted features, deep learning (DL) methods [45] can automatically extract and learn complex feature representations. Since the seminal work of Krizhevsky et al. [46], which achieved exceptional image classification performance by training a convolutional neural network (CNN) with efficient computation resources, deep learning is one of the most rapidly evolving fields and has been successfully applied to numerous computer vision problems. To this end, Luo et al. [47] developed a smoke detection algorithm based on the motion characteristics of smoke and a CNN. Firstly, they identified the candidate regions based on the background dynamic update and dark channel a priori method [48]. Then, the features of the candidate region were extracted automatically by aCNN consisting of five convolutional layers and three fully connected layers. In [49], the authors combined deep learning and handcrafted features to recognize the fire and smoke areas. For static features, the AlexNet architecture was adapted, while for dynamic features an adaptive weighted direction algorithm was used. Moreover, Sharma et al. [50] used optical images and re-tuned two pre-trained CNNs, based on VGG16 and ResNet50 backbones to distinguish images that contain fire and images that do not. It is worth mentioning that for the training, they createdan unbalanced dataset including more non-fire images. Zhang et al. [51] proposed deep CNNs forforest fire detection in a cascaded fashion. Firstly, they trained a full image fire classifier to decidewhether the image contains the fire or not and then applied a fine-grained patch classifier to localize the fire patches within this image. The full image classifier is a deep CNN that has been fine-tuned from AlexNet and the fine-grained patch classifier is a two-layer fully connected neuralnetworks trained with the upsampled Pool-5 features. Muhammad et al. [52], inspired byGoogleNet architecture and proposed a fine-tuned fire detection CNN model for surveillance videos, while Shen et al. [53] used an optimized YOLO model for flame detection from video frames. Frizzi et al. [54] built a simple CNN consisting of nine layers. The architecture of this model was similar to LeNet-5 including dropout layers and used a leaky rectified linear unit (ReLU) activation function. Muhamad et al. [55] proposed a fine-tuned CNNs architecture based on theSqueezeNet model and developed a feature map selection algorithm for fire segmentation and background analysis. In [56], the authors combined AlexNet as a baseline architecture and the internet of multimedia things (IoMT) for fire detection and disaster management. The developedsystem introduced an adaptive prioritization mechanism for cameras in the surveillance system allowing high-resolution cameras to be activated to confirm the fire and analyze the data in real-time. Furthermore, Dunning's and Breckon [57] used low-complexity CNN architectural variants and applied a super pixel localization approach aiming to reduce the computational performance offering up to 17 fps processing time.

Since the number of publicly available wildfire datasets is still limited, Sousa et al. [58] proposed a fire detection method based on data augmentation and transfer learning. A method that had been pre-trained on the ImageNet Inception-v3 model was retrained and evaluated using ten- fold cross-validation on the Corsican Fire Database [59]. Extending deep learning approaches, Barmpoutis et al. [60] combined the power of faster region-based convolutional neural network(R-CNN) with multidimensional dynamic texture analysis based on higher-order LDSs aiming theearly forest fire detection. A modified faster R-CNN and a 3D CNN were combined in [61]. To thatend, the faster R-CNN with non-maximum annexation was utilized to realize the smoke target location based on static spatial information and then a 3D CNN was used for smoke recognition by combining dynamic spatial–temporal information. Jadon et al. [62] developed the FireNet convolution neural network using a standard fire dataset and a self-proposed dataset, achieving an encouraging performance in terms of a series of evaluation metrics. Zhang et al. [63] trained a faster R-CNN for forest smoke detection by creating synthetic smoke images and achieved greatperformance when tested on real smoke images. Moreover, in [64] the authors extracted spatialfeatures through a faster R-CNN for the detection of the suspected regions of fire (SroFs) and non-fire. Then, the features of the detected SroFs in successive frames were used by a long short-term memory (LSTM) for them to identify whether there is a fire or not in a short-term period. Finally, a majority voting method and the exploitation of fire dynamics were used for the final decision. Shi et al. [65] inspired by the idea of R-CNN and combined image saliency detection andconvolutional neural networks. More specifically, they utilized the pixel-wise image saliency aggregating (PISA) method [66] to identify the candidate regions and then classified them into fire or non-fire regions.

Instead of extracting bounding boxes, Yuan et al. [67] used a two-path encoder-decoder fully convolutional network (FCN) for visual smoke segmentation. FCNs can achieve end-to-end pixel-wise segmentation so the precise location of smoke can be identified in images. They also created synthetic smoke images instead of labeling the real smoke images manually for training and then tested the network on both synthetic and real videos. Cheng et al. [68] proposed a smoke detection model using Deeplabv3+ and a generative adversarial network (GAN). The smoke pixelswere first identified by fusing the result Deeplabv3+ and the heatmap of smoke based on HSV features. Then, a GAN was employed for predicting the smoke trend heatmap based on the space–time analysis of the smoke videos. Finally, in [69] the authors used a two-stage training ofdeep convolutional GANs for smoke detection. This procedure included a regular training step ofa deep convolutional (DC)-GAN with real images and noise vectors and a training step of the discriminator separately using the smoke images without the generator.

2.2. Unmanned Aerial Vehicles

Terrestrial imaging systems can detect both flame and smoke, but in many cases, it is almost impossible to view, in a timely manner, the flames of a wildfire from a ground-based camera or a mounted camera on a forest watchtower. To this end, autonomous unmanned aerial vehicles (UAVs) can provide a broader and more accurate perception of the fire from above, even in areas that are inaccessible or considered too dangerous for operations by firefighting crews. Either fixed or rotary-wing UAVs cover wider areas and are flexible, allowing the change of monitoring

area, but they are affected by weather conditions and have limited flight time. UAVs mostly use ultra-high-resolution optical or infrared charge-coupled device (CCD) cameras to capture images as well as other sensors for navigation, such as global positioning system (GPS) receivers or inertial measurement units (IMUs).

2.2.1. Traditional Methods

The first attempts for aerial fire detection began around 1920 when planes were used for forest fire detection as a result of their unsuccessful deployment for the extinguishing of fires [70]. In 1986, Stearns et al. [71] captured IR images by the Flying Infrared Signatures Technology Aircraft of the

U.S. Air Force Geophysics Laboratory and described a spatial and spectral analysis methodology to provide wildfire detection and monitoring for fire control. Similarly, Den Breejen et al. [72] used a single manned aerial vehicle for forest fire detection and tracking; however, although the operation of manned aerial vehicles is safer in busy airspace around fire [12], these vehicles are typically large and require increased operational costs making them a less useful tool for fire detection.

In recent times, the deployment of UAVs is considered to be a better option for the task of forest fire detection. More specifically, to achieve forest fire detection and tracking, Yuan et al. [73] used median filtering for noise reduction, color analysis based on CIELAB color space, Otsu threshold for fire segmentation, and blob counting. More recently, in [74] they used visual images captured by an optical camera of an unmanned aerial vehicle. Then, two color spaces, namely, RGB and HIS were chosen as inputs of a fuzzy logic rule and an extended Kalman filter was employed to adapt environmental condition variations and to perform smoke detection. Extending the color-based methods in [75,76] fire flame and smoke pixels are segmented using both color and motion characteristics. For the estimation of color features, they utilized three color spaces RGB, YCbCr, and HIS, whereas for the extraction of motion characteristics they noted that flames have turbulent movement or disordered characteristics. Thus, an optical flow algorithm was used to examine the motion characteristic of forest fires and extract fire motion pixels using dynamic background analysis.

Aiming to identify the fire location in terms of latitude, longitude, and altitude in [77], the authors used a DJI F550 hexacopter and applied two coordinate system transformations between the body-fixed frame, namely north-east-down frame (NED) and Earth-centered Earth-fixed (ECEF) frame. Then, a rule-based color model combining RGB and YCbCr color spaces was used for the identification of fire pixels. A fire simulation platform based on the Unity game engine and robot operating systems (ROS) was developed by Esfahlani [78]. The video data were collected through a monocular camera and navigation relied on a simultaneous localization and mapping (SLAM) system. A fire detection algorithm based on color, movement attributes, temporal variation of fire intensity, and its accumulation around a point was deployed. Finally, a mixed reality (MR) system incorporating physical and virtual elements was adopted to visualize and test the developed system.

Sudhakar et al. [79] proposed a method for forest fire detection through UAVs equipped with an optical and an infrared camera. They used a LAB color model and a motion-based algorithm followed by a maximally stable extremal regions (MSERs) extraction module. For improved presentation, the extracted forest fire detections are joined with landscape information and meteorological data. In [80] two types of UAVs, a fixed-wing drone and a rotary-wing drone equipped with optical and thermal cameras were used. As soon as the fixed-wing drone detects a fire, the rotary-wing drone will fly at a much lower altitude (10 to 350 m) compared to a fixed-wing UAV (350 to 5500 m), thus having better and more detailed visibility of the area and reducing false alarms through a neural network. Chen et al. [81] used optical and infrared sensors and data to train a CNN first for smoke detection and then for flame detection. In [82], the authors developed a system consisting of a central station and several aerial vehicles equipped with infrared or visual cameras, aiming to increase the coverage area. For fire detection, they applied a threshold for fire segmentation and then performed color and fire contour analysis.

2.2.2. *Deep Learning Methods*

Zhao et al. [83] used a UAV equipped with GPS and deployed a saliency detection algorithm for localization and segmentation of the fire area in aerial images. Then, a 15 layered deep convolutional neural network architecture was employed for both low and high-level fire feature extraction and classification. Tang et al. [84] captured 4K data using a ZenMuse XT2 dual vision sensor and applied an adaptive sub-region select block to detect fire candidate areas in 4K resolution images. Then, a YOLOv3 backbone architecture was used for fire detection. Jiao et al. [85] used a UAV to capture and transmit images to the ground station in real-time deploying a YOLOv3 network for fire detection. Furthermore, they deployed a UAV equipped with a visible and an infrared camera for image acquisition [86]. The onboard computer carried by UAV can perform local image processing and mission planning through a YOLOv3-tiny architecture. In addition, a ground station receives images and location information of fire spots, contributing to the detection of forest fires. Furthermore, it provides operational commands to the UAV for path planning and re-planning. Integrating fog computing and CNNs, Srinivas and Dua [87] employed a UAV to reduce the false alarm rates towards the task of forest fire detection at an early stage. More recently, Barmpoutis, et al. [88,89] used an optical 360-degree complementary metal-oxide-semiconductor (CMOS) camera mounted on a UAV to capture an unlimited field of view images. More specifically, they converted the equirectangular raw data to cubemap and stereographic projections, respectively. Then, they used deep neural networks and exploited fire dynamic textures aiming to reduce false alarms that are caused due to clouds, sunlight reflections, and fire/smoke-colored objects. Experimental results demonstrate the great potential of the proposed system for both flame and smoke detection.

2.3. *Spaceborne (Satellite) Systems*

Recently, mainly due to the large number of satellites launched and the decrease of associated costs, there are many research efforts to detect forest wildfires from satellite images. Specifically, a set of satellites were designed for Earth observation (EO, e.g., environmental monitoring or meteorology). Depending on their orbit, satellites can be broadly classified into various categories, each having their advantages and disadvantages. The most important categories

include: (a) the geostationary orbit (GEO), which is a circular orbit with an altitude of 35,786 kilometers and zero inclination, so that the satellite does not move at all relative to the ground, providing a constant view of the same surface area,

(b) the low Earth orbit (LEO), which has an altitude of 2000 km or less, requires the lowest amount of energy for satellite placement and provides high bandwidth and low communication latency, (c) the polar sun-synchronous orbit (SSO), which is a nearly polar orbit that passes the equator at the same local time on every pass. Most EO satellites are in specific low Earth polar SSO orbits, whose altitude and inclination are precisely calculated so that the satellite will always observe the same scene with the same angle of illumination coming from the Sun, so shadows appear thesame on every pass.

Data from sun-synchronous satellites have high spatial resolution but low temporal resolution, whereas geostationary satellites have high temporal resolution but low spatial resolution. Some satellites of the first category, like Landsat or Sentinel satellites, have a large revisit time (eight-day repeat cycle for LandSat-7/8 and approximately 2–3 days at mid-latitudes for Sentinel 2A/2B). Hence, they are unsuitable for real-time active forest fire detection, but only for less time-sensitive tasks, e.g., burnt area estimation, and therefore their studies fall within the scopeof this paper.

2.3.1. *Fire and Smoke Detection from Sun-Synchronous Satellites*

Imaging sensors in sun-synchronous satellites include three multispectral imaging sensors, namely advanced very-high-resolution radiometer (AVHRR) [90], moderate resolution imaging spectroradiometer (MODIS) [91], and visible infrared imaging radiometer suite (VIIRS) [92,93], whose data have also been used for wildfire detection. The advanced very-high-resolution radiometer (AVHRR/3) is a multipurpose imaging instrument that measures the reflectance of the Earth and has been used for global monitoring of cloud cover, sea surface temperature, ice, snow, and vegetation cover characteristics [90]. AVHRR instruments are or have been carried bythe National Oceanic and Atmospheric Administration (NOAA) family of polar-orbiting platforms (polar-orbiting operational environmental satellite—POES) and European Meteorological Operational (MetOp) satellites. The instrument provides six channels, three in the visible/near-infrared region and three thermal infrared channels, with 1 km spatial resolution. The moderate resolution imaging spectroradiometer (MODIS), onboard the National Aeronautics Space Administration (NASA) EO Terra and Aqua satellites that have a revisit time of 1–2 days, capture data in 36 spectral bands ranging in wavelengths from 0.4 to 14.4 µm and at varying spatial resolutions (2 bands at 250 m, 5 bands at 500 m, and 29 bands at 1 km). MODIS was succeeded by the visible infrared imaging radiometer suite (VIIRS) instrument onboard the Suomi National Polar-orbiting Partnership (NPP) and NOAA-20 weather satellites. The instrument provides 22 different spectral bands, i.e., 16 moderate-resolution bands (M-bands, 750 m), 5 imaging resolution bands (I-bands, 375 m), and 1 day/night panchromatic band (750 m).

Traditional Methods

x

These imaging sensors have also been extensively applied for near-real-time wildfire detection. For instance, in [94], Sayad et al. combined big data, remote sensing, and data mining algorithms (artificial neural network and SVM) to process big data collected from MODIS images and extract insights from them to predict the occurrence of wildfires. More specifically, they used pre-processed MODIS data to create a dataset based on three parameters related to the state of the crops: namely normalized difference vegetation index (NDVI), land surface temperature (LST), and thermal anomalies. For wildfire prediction, they used two different supervised classification approaches based on neural networks and SVM, achieving good prediction accuracies, i.e., 98.32% and 97.48%, respectively. Results were assessed using several validation strategies (e.g., classification metrics, cross-validation, and regularization) and comparisons with other wildfire prediction models, demonstrating the efficiency of the model in predicting the occurrence of wildfires.

Several papers deal with the problem of smoke detection based on MODIS data, which is a very challenging problem given its strong similarity with clouds, haze, and other similar phenomena. Shukla et al. [95] proposed an algorithm for automatic detection of smoke using MODIS data, which was based on a multiband thresholding technique for discriminating between smoke plumes and clouds. Results suggested that the algorithm was able to isolate smoke pixels in the presence of other scene types, such as clouds, although it performed better in identifying fresh dense smoke as compared to highly diffused smoke. Similarly, Li et al. [96] proposed an approach to automatically separate smoke plumes from clouds and background by analyzing MODIS data. Specifically, a previous approach proposed by Li et al. [97] for the AVHRR sensor was improved based on spectral analysis among the smoke, cloud, and underlying surface using MODIS data. Specifically, a multi-threshold method was used for extracting training sample sets to train a back-propagation neural network (BPNN) to discriminate between three classes: (smoke, cloud, and underlying surface). Results using MODIS data of several forest fires occurred in different places and different dates were satisfactory. Advantages include the ability of the algorithm to detect smoke plumes in different seasons using seasonal training data sets, as well as that it provides quantitative and continuous outputs of smoke and other objects. Many researchers used active fire products derived from these sensors to assess various other proposed algorithms. Hally et al. [98] examined the performance of a threshold algorithm against commonly used products such as the VIIRS active fire product, to determine the completeness of anomaly capture. Specifically, the study considers two commonly used active fire products: the MODIS Collection 6 (MOD/MYD14) 1 km active fire product as outlined in Giglio et al. [99] and the VIIRS 375 m (VNP14IMG) active fire product described in Schroeder et al. [93]. In both cases, the geographic position of the detected hotspots, as well as the time of satellite overpass, were used. Also, Wickramasinghe et al. [100] compared the Advanced Himawari Imager—Fire Surveillance Algorithm (AHI-FSA) across the Northern Territory of Australia (1.4 million km2) over ten days with the well-established active fire

products from satellites: MODIS and VIIRS.

Finally, the Chinese HuanJing sun-synchronous satellites ("HuanJing" means "environment" in Chinese) are satellites for disaster and environmental monitoring that are capable of visible, infrared, multi-spectral, and synthetic aperture radar imaging. Lin et al. [101] presented a spatio–

temporal model (STM) based forest fire detection method that uses multiple images of the inspected scene based on Huanjing-1B satellite images. A comparison of detection results demonstrated that the proposed algorithm is useful to represent the spatio–temporal information contained in multi-temporal remotely sensed data.

Deep Learning Methods

Deep Learning methods have also been recently applied for fire and smoke detection from multispectral satellite images. Ba et al. [102] presented a new large-scale satellite imagery dataset based on MODIS data, namely USTC_SmokeRS, consisting of 6225 satellite images from six classes (i.e., cloud, dust, haze, land, seaside, and smoke) and covering various areas/regions over the world. Using this dataset, they evaluated several state-of-the-art deep learning-based image classification models for smoke detection and proposed *SmokeNet*, a new CNN model that incorporated spatial- and channel-wise attention in CNN to enhance feature representation for scene classification. Also, Priya et al. [103] used a dataset of 534 RGB satellite images from different sources, including MODIS images from the NASA Worldview platform and Google. An effective approach using an Inception-v3 CNN framework and transfer learning was used for fire and non-fire image classification. Then, the fire regions were extracted based on thresholding and local binary patterns.

2.3.2. Fire and Smoke Detection from Geostationary Satellites

Regarding satellite imagery from geostationary satellites, important work for fire and smoke detection has already been performed using the advanced Himawari imager (AHI) sensor of the Himawari-8 weather satellite. Himawari 8 is a new generation of Japanese geostationary weather satellites operated by the Japan Meteorological Agency. AHI-8 has significantly higher radiometric, spectral, and spatial resolution than its predecessor.

Regarding Europe and the US, two additional sensors that are installed in geostationary satellites are the European Space Agency (ESA) Meteosat second generation (MSG, a satellite series)-spinning enhanced visible and infrared imager (SEVIRI) sensor and the NASA geostationary operational environmental satellite (GOES)-16 advanced baseline imager (ABI) sensor. The MSG-SEVIRI geostationary sensor is a 50 cm diameter aperture, line-by-line scanning radiometer, which provides image data in 12 spectral channels (four visible and near-infrared (NIR), including a broadband high resolution (1 km) visible channel, and eight thermal IR with a resolution of 3 km) with a baseline repeat cycle of 15 min. GOES-16 is the first of the GOES-R series of the geostationary operational environmental satellite (GOES) operated by NASA and the NOAA. The advanced baseline imager (ABI) is its primary instrument, providing high spatial and temporal resolution imagery of the Earth through 16 spectral bands at visible and infrared wavelengths.

Traditional Methods

Hally et al. [98] extended previous work by the same authors Hally et al. [104] using AHI sensor data from the Himawari geostationary satellite in the application of a multi-temporal method of background temperature estimation, known as the broad area training (BAT). This method

involves a two-step process for geostationary data: a preprocessing step, where AHI Band 7 images are aggregated and then a fitting step, where this spatially aggregated data are used in individual pixel fitting using a single value decomposition (SVD) process. These fittings at the pixel level can then be compared to the raw brightness temperature data as measured by the satellite sensor, to identify thermal anomalies such as those caused by an active fire. Results are seen to compare favorably to active fire products produced by low Earth orbit satellite data during the period of study. Fatkhuroyan et al. [105] perform a study of data from fires in Sumatera and Kalimantan regions in August, September, and October 2015 and concluded that smoke detection and monitoring is feasible using pseudo-RGB images consisting of one visual channel and two near-infrared channels. A limitation revealed by this study is that Himawari-8/AHI is a passive sensor that very dependent on the reflection of solar radiance, so it can only monitor the forest fire during the day-time. Xu et al. [106] investigated the feasibility of extracting real-time information about the spatial extents of wildfires using the Himawari-8 satellite. The algorithm is based on previous work using the MODIS sensor: it first identifies possible hotspots and then eliminates false alarms by applying certain thresholds, similar to Giglio et al. [99]. False alarms are then rejected by cloud, water, and coast tests based on the additional bands and comparison with neighboring pixels. Results demonstrated that fire detection is robust to smoke and moderate cloud obscuration and sensitive enough for early detection of wildfires.

Typically, only temporal-based fire detection algorithms are used for geostationary orbital sensors, detecting the fire by analyzing multi-temporal changes of brightness temperature (BT). On the other hand, polar-orbiting platforms, use spatial-based fire detection algorithms, which are commonly classified either "fixed-threshold" or "contextual". Aiming to combine the merits of both approaches, Xie et al. [107] presented a spatio–temporal contextual model (STCM) that fully exploits geostationary data's spatial and temporal dimensions using data from Himawari-8 Satellite. They applied an improved robust fitting algorithm to model each pixel's diurnal temperature cycles (DTC) in the middle and long infrared bands. For each pixel, a Kalman filter was used to blend the DTC to estimate the true background brightness temperature.

Significant research results have also been produced using data from the GOES ABI and MSG SEVIRI instruments. A multi-temporal change-detection technique, namely robust satellite techniques for fires detection and monitoring (RST-FIRES) using data from the MSG-SEVIRI sensor. Filizzola et al. [108] was seen to be very efficient for the timely detection of even small/short-living fire incidents. Furthermore, Di Biase et al. [109] updated the satellite fire detection (SFIDE) algorithm, previously proposed by the same authors Laneve et al. [110] to reduce the false alarm rate. Specifically, they improved the estimation of the reference temperature used to define a fire pixel, the cloud mask accuracy, and the exploitation of the high refresh rate of the images to implement several tests for more accurate detection of forest fires. In Hall et al. [111], both satellite imaging sensors (GOES ABI and MSG SEVIRI) were found to be very efficient in detecting active fire incidents. Additional sensing systems providing such broad spatial coverage and favoring improved geostationary satellite fire data consistency across regions could further improve performance. Reference fire data were derived from Landsat-8 Operational Land Imager (OLI) 30 m imagery using the Schroeder et al. [112] Landsat-8 OLI automated fire detection algorithm.

Deep Learning Methods

Very recently, Larsen et al. [113] presented a deep FCN for predicting fire smoke in satellite imagery in near-real-time (NRT) using data from the Himawari-8/AHI sensor. Also, Phan et al. [114] proposed a novel remote wildfire detection framework based on GOES-16 sensor imagery, which contains three distinct stages: (i) a streaming data processing component to purify and examine raw image data for ROI's, (ii) an early wildfire prediction component using deep learning architectures to grab spatial and spectral designs for more accurate and robust detection, and (iii) a streaming data visualization dashboard for potential wildfire incidents.

2.3.3. *Fire and Smoke Detection Using CubeSats*

A recent trend in remote sensing from satellites is using "Cubsats", i.e., miniaturized satellites that typically weigh between 1 and 10 kg and follow the popular 'CubeSat' standard [115], which defines the outer dimensions of the satellite within multiple cubic units of $10 \times 10 \times 10$ cm and can accommodate small technology payloads to perform different scientific research or commercial functions and explore new space technologies. Technically, it is easier for CubeSats to function in the LEO-zone due to their unique characteristics. More than 1100 CubeSats have been successfully launched by several universities and companies worldwide, as of January 2020.

The latest advances in satellite imagery had allowed CubeSats to rapidly discover wildfires. Barschke et al. (2017) [116] described a nanosatellite called TUBIN (Technische Universität Berlin Infrared Nanosatellite), which was designed to validate an infrared microbolometer for wildfire remote sensing. Another constellation of four 6U Cubesats for monitoring forest fires and other natural disasters was proposed in Africa and Asia [117]. The payload is an optical sensor with three spectral bands (green, red, and near-infrared) with a revisit time of 72 h. Shah et al. [118] proposed a system consisting of a constellation of nanosatellites equipped with multi-spectral visible to Infrared (IR) cameras and a ground station, which will allow all surface points on the planet to be revisited at least once in an hour. Capturing a surface location with high resolution in MWIR and LWIR allows for the precise estimation of the thermal output of the surface. Simulations indicated that a fire of about four hundred square meters can be detected using a payload of a multispectral IR camera measuring incident power in two thermal infrared bands (mid-wave and long-wave). The system will use onboard data processing, enabling an early wildfire warning within 30 min and minimizing bandwidth requirements. Additionally, compressed raw images can be transmitted to the ground station to provide global thermal data updated every 90 min. The first satellite is planned for launch in late 2020 with the data available for research purposes.

3. Comparative study

Three categories of early fire and smoke detection systems have been analyzed and compared (Table 1) thoroughly in this literature review paper, namely terrestrial, unmanned aerial vehicles, and satellite-based systems. In general, terrestrial systems tend to be more efficient in terms of accuracy and response time to wildfire incidents. Furthermore, these systems offer high spatial resolution depending on the camera resolution and the viewing angle/distance; however, their

coverage is limited when compared to the other two solutions, as the cameras are placed in fixed positions and additional limitations may apply (e.g., occlusions).

On the other hand, aerial-based systems gained recently a lot of attention due to the rapid development of UAV technology. Such systems provide a broader and more accurate perception of the fire, even in regions that are inaccessible or considered too dangerous for fire-fighting crews. In addition, UAVs can cover wider areas and are flexible, in the sense that they monitor different areas, as needed. Recent technological achievements have led to better camera resolutions offering high spatial resolution, wider field of view, and better battery autonomy. The latest UAVs are equipped with both visible and infrared cameras, improving the detection accuracy and allowing night operation; however, they are affected by weather conditions and, in many cases, their flight time is limited.

Table 1. Multi spectral imaging systems and their characteristics.

	(Satellite)-Sensor	SpectralBands	Accesstothe Data	Specs/Advantages/Limitations	Spatial Scale	SpatialResolution	DataCoverage	AccuracyRange
Terrestrial	**Optical**	Visible spectrum	Both web cameras and image and video	Easy to operate, limited field of view, need to be carefully placed in order to ensure adequate visibility.	Local	Very high spatial resolution (centimeters)depending on ca mera resolution and distanc e between the	Limited coverage depending the specific task of	85%–100% [35,40,58,60]
	IR	Infrared spectrum						
	Multimodal	Multispectral	Are available			Camera and the event	each system	
Aerial	**Optical**	Visible spectrum	Limited numberofaccess iblepublishedda ta	Broaderandmoreaccuratepercep tionofthefire,coverwiderareas,fl exible,affectedbyweatherconditi ons,limitedflighttime.	ocal—Regional	HighspatialresolutionL dependingonflight altitude,cameraresolution anddistancebetweenthec ameraandtheevent	Coverage of hund redhectaresdep endingonbatter ycapacity.	70%–94.6% [75,86,89]
	IR	Infrared spectrum						
	Multimodal	Multispectral						
Satellite	**Terra/Aqua-MODIS** [118]	36(0.4–14.4μm)	Registration Required (NASA)	Easilyaccessible,limitedspatialr esolution,revisittime:1–2days	Global	0.25km(bands1–2)0.5km (bands3–7) 1km(bands8–36)	Earth	92.75%–98.32% [94–96,99,102]
	Himawari-8/9—AHI-8 [119]	16(0.4–13.4μm)	Registration Required/ (Hexaware Cloud)	Imaging sensors with high radio spectral, and temporal resolution. 10 min (Fulldisk), revisit time:5 min For are Asian, Japan/Australia)	Regional	0.5km or1 km for visible and near-infrared bandsand2kmforinfraredb ands	East Asiaan dW Eastern Pacific	75%–99.5% [98,100,104–107,113]
	MSG—SEVIRI[120]	12(0.4–13.4μm)	Registration Required (EUMETSAT	Low noise in the long- Wave IR channels, tracking of dust storms in near-real-time, Susceptibility of the larger field of View to contamination by cloud 15min	Regional	1kmforthe high-resolution visible channel 3kmfortheinfraredandthe3 0ther visible channels high temporal resolution butrelatively low spatial resolution, and delay sindatadeliv ery,revisittime:5–15min	Atlantic Ocean, Europeand Africa	71.1%–98% [108–111]
	GOES-16ABI[121]	16(0.4–13.4μm)	Registration Required (NOAA)	Infrared Resolution sallow the detection of much smaller wildly and fires with			Regional 0.5	kmfo rthe0 .64μ m visib le chan

nel

1 km for other visible/n ear-IR
2kmforbands>2µm

Western Hemisphere (Northland
South America
)

94%–98%
[111,114]

Table1. *Cont.*

(Satellite)-Sensor	Spectral Bands	Access to The Data	Specs/Advantages/Limitations	Spatial Scale	Spatial Resolution	Data Coverage	Accuracy Range
Huan Jing (HJ)-1B—WVC(Wide View CCD Camera)/**IRMSS** (Infrared Multispectral Scanner)[122]	WVC:4 (0.43–0.9μm) IRMSS:4 (0.75–12.5μm)	Registration Required	Lack of anon board calibration System to track HJ-1 sensors' on-orbit behavior throughout the Life of the mission, revisit time: 4days	Regional	WVC:30m IRMSS:150–300m	Asian and Pacific Region	94.45%[101]
POES/Met Op—AVHRR [123]	6(0.58–12.5μm)	Registration Required (NOAA)	Coarse spatial resolution, revisit time:6h	Global	1.1kmby4kmatnadir	Earth	99.6%[97]
S-NPP/ NOAA-20/NOAA— VIIRS-375m[124,125]	16 M-bands (0.4–12.5μm) 5I-bands (0.6–12.4μm) 1DNB (0.5–0.9μm)	Registration Required (NASA)	Increased spatial resolution, Improved mapping of large fire perimeters, revisittime:12h	Global	0.75km(M-bands) 0.375km(I-bands) 0.75 km (DNB)	Earth	89%–98.8%[93]
CubeSats (data refer to a Specific design from [126])	2:MWIR (3–5μm)and LWIR(8–12μm)	Commercial access planned	Small physical size, reduced cost, Improved temporal resolution/response time, Revisit time: less than 1 h.	Global	0.2km	Wide coverage In orbit	The first satellite is Planned for launch in late2020

4. Methodology:

Currently, available VFD algorithms mainly focus on the detection and analysis of smoke and flames inconsecutive video images. In early articles, mainly flame detection was investigated. Recently, the smoke detection problem is also considered.The reason for this can be found in the fact that smoke spreads faster and in most cases willoccur much faster in the field of view of the cameras. In wild-fire applications, it may not be even possible toobserve flames for a long time. The majority of the state-of-the-art de-section techniques focus on the color and shape characteristics together with the temporal behavior of smoke and flames. How-ever, due to the variability of shape, motion, transparency,colors, and patterns of smoke and flames, many of the existing VFD ap-preaches are stillvulnerable to false alarms. Due to noise, shadows, illumination changes, and other visual artifacts in recorded video sequences, developing are liable detection system is a challenge to the image processing and computer vision community.

With today's technology, it is not possible to have a fully available VFD system without ahuman operator. However, current sys-teams are invaluable tools for surveillance operators. It is also our strong life that combining multimodal video information using both visible and infrared (IR) technology will together higher detection accuracy. Each sensor type has its specific limitations, which can become presented by other types of sensors. Although it would be desirable to develop a firedetection system that could operate on the existing closed-circuit television (CCTV) equipment without introducing any additional cost. However, the cost ofusing multiple video sensors does not outweigh the benefit of multi-modal fire analysis. The fact that IR manufacturers also ensure a decrease in the sensor cost soon, fully opens the door to multimodal video analysis. VFD camera scans also be used to extract useful related information, such as the presence of people caught in the fire, fire size, fire growth, smoke direction, etc.

Video fire detection systems can be classified into various sub-categories according to

   a. The spectral range of the camera used,
   b. The purpose (flame or smoke detection),
   c. The range of the system.

4.1. Video fire detection invisible/visual spectral range:

Over the last few years, the number of papers about visual fire detection in the computer vision literature is growing exponentially. As is, this relatively new subject in vision research is in full and has already produced promising results. However, this is not a completelysolved problem as in most computervision problems. The behavior of smoke and flames of controlled fire differs with distance and illumination. Furthermore, cameras are not color and/or spectral measurement devices.They have differ-ent sensors and color and illumination balancing algorithms.They may produce different images and videos for the same scene be-cause of their internal settings and algorithms.

4.2. Color detection

Color detection was one of the first detection techniques used in VFD and is still used inalmost all detection methods. The majority of the color-based approaches in VFD make use of RGB color space, sometimes in combination with HSI/HSV saturation[10,24,27,28]. The main reason for using RGB is that almost all visible range cameras have sensors detecting video in RGB format and there is the obvious spectral content associated with this color space. It is reported that RGB values of flame pixels are in red-toyellow color range indicated by the rule $(R>G>B)$ as showninFig.1. Similarly, in smoke pixels, R, G and B values are very close to each other. More complex systems use rule-based techniques such as Gaussian smoothed color histograms[7], statistically generated color models [15], and blending functions[20]. It isobvious that color cannot be used by itself to detect fire because of the variability in color, density, lighting,and background. However,the color information can be used as a part of a more sophisticated system. For example, chrominance decrease is used in smoke detection schemes of [14] and [2]. Luminance value ofsmoke regions should be high for most smoke sources. On the other hand, the chrominance values should be very low.

The second YUV color space areas follows:

*Condition*1: $Y>T_Y$,

*Condition*2: $|U-128|<T_U$ and $|V-128|<T_V$,

where Y, U, and V are the luminance and chrominance values ofa particular pixel, respectively. The luminance component Y takesvaluesintherange0, 255in an 8-bit quantized image and the mean values of chrominance [l]channels, U and V are

increased to 128 so that they also take values between 0 and 255. The thresh- oldsT_Y, $T_U$and$T_V$areexperimentallydetermined[37].

4.3. **Moving object detection**

Moving object detection is also widely VFDbecause flame sand smoke is moving objects. To determine if the motion is due to smoke oran ordinary moving object, further analysis of moving regions in the video is necessary. Well-known moving object detection algorithm are background(BG) subtraction methods [16 ,21,18 ,14, 13,17, 20,22,27,28,30,34], temporal differencing[19], and optical flow analysis [9,8,29]. They can all be used as part of a VFD system.

Table 2

State-of-the-art: underlying techniques (PART1:2002–2007).

Paper	Color detection	Moving object detection	Flicker/energy (wavelet)analysis	Spatial difference analysis	Dynamic texture/pattern analysis	Disorder analysis	Sub blocking	Training (models, NN, SVM, …)	Clean-up post-processing	Localization/analysis	Flame detection	Smoke detection
Phillips[7],2002	RGB		X	X				X	X		X	
Gomez-Rodriguez [8],2002		X	X			X						X
Gomez-Rodriguez [9],2003		X	X			X						X
Chen[10],2004	RGB/HSI	X				X					X	X
Liu[11],2004	HSV		X			X					X	
Marbach[12], 2006	YUV		X			X					X	
Toreyin[13],2006	RGB	X	X	X							X	
Toreyin[14],2006	YUV	X	X			X						X
Celik[15],2007	YCbCr/RGB										X	X
Xu[16],2007		X	X			X					X	X

Table 3

State-of-the-art: underlying techniques (PART2:2007–2009).

Paper	Color detection	Moving object detection	Flicker/energy (wavelet)analysis	Spatial difference analysis	Dynamic texture/pattern analysis sis	Disorder analysis	Sub blocking	Training (models, NN, SVM, …)	Clean- up post processing	Localization/analysis	Flame detection	Smoke detection
Celik[17],2007	RGB	X				X		X	X		X	
Xiong[18],2007		X	X			X						X
Lee[19],2007	RGB	X						X	X		X	X
Calderara[20], 2008	RGB	X	X				X	X				X
Piccinini[21], 2008	RGB	X	X					X				X
Yuan[22],2008	RGB	X				X	X					X
Borges[23],2008	RGB					X					X	
Qi[24],2009	RGB/HSV		X	X					X		X	
Yasmin[25],2009	RGB/HSI	X				X	X			X		X
Gubbi[26],2009			X				X	X				X

In background subtraction methods, it is assumed that the camera is stationary. In Fig. 2, a background subtraction-based motion detection example is shown using the dynamic background. This Gaussian Mixture Model based approach model was used in many of the articles listed in Table-2,3.
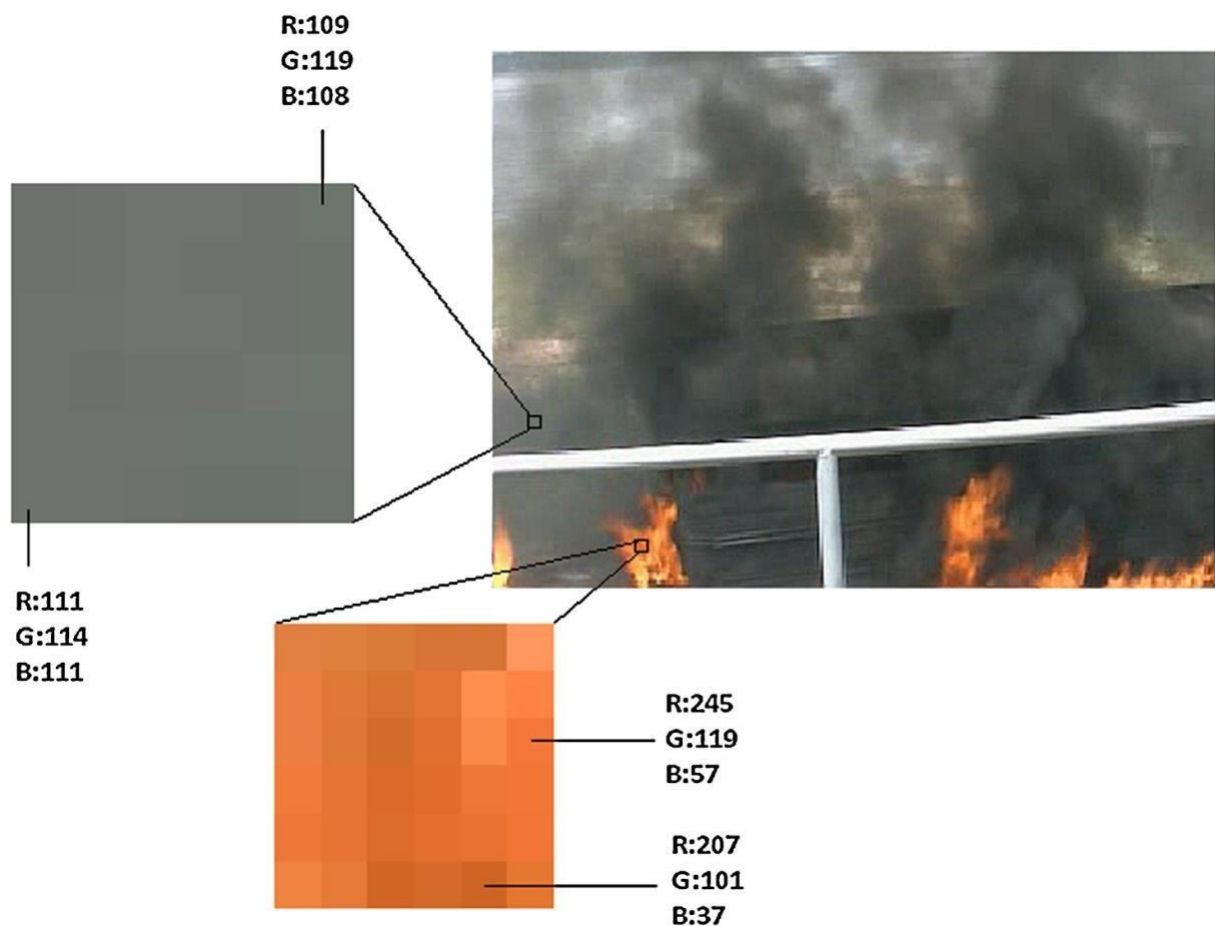
Fig.1. Color detection: smoke region pixels have color values that are close to each other. Pixels of flame regions lie in the thread yellow range of RGB color space with $R>G>B$. (For interpretation of there color in this figure legend, the reader is referred to the web version of this article.)
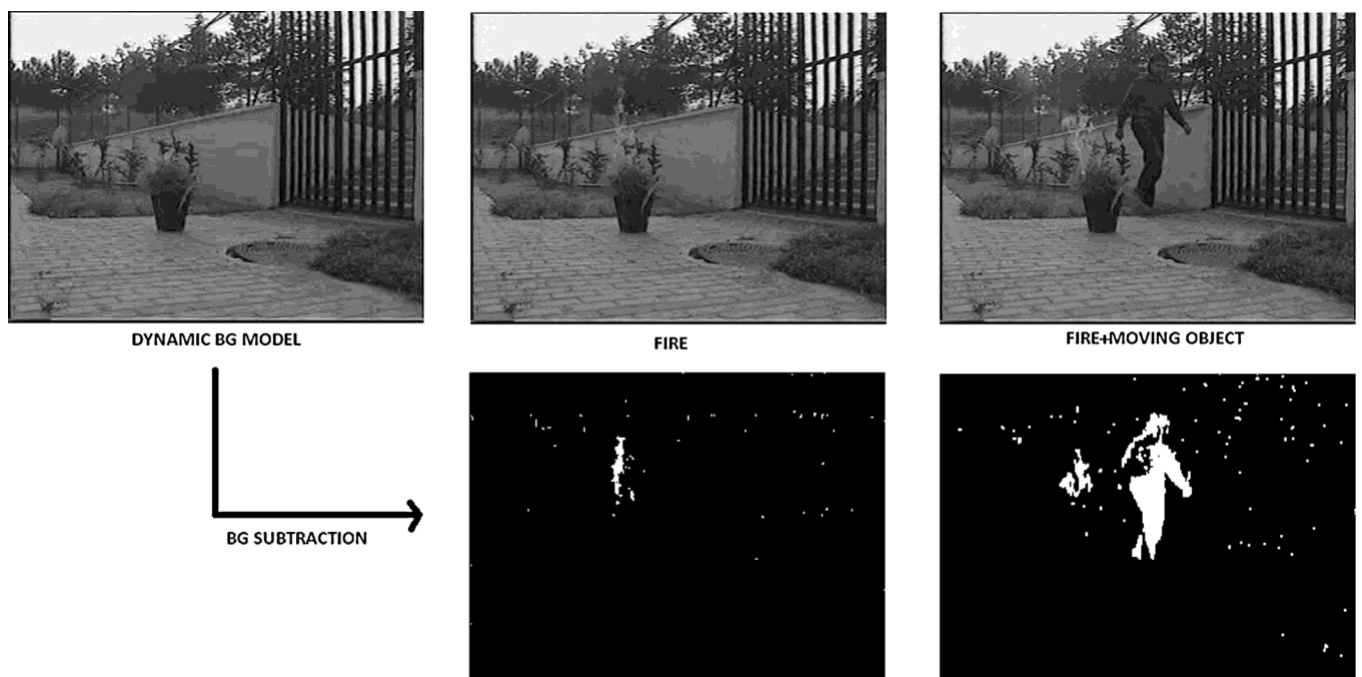
Fig.2. Moving object detection: background subtraction using dynamic background del.

4.4. **Wild fire smoke detection using IR camera**

Johnson's criteria are about "seeing a target" in an infrared cam-era. The first criterion defines detection: In order to detect an object its critical dimension needs to be covered by1.5 ormore pixel sin the captured image. Therefore wild fires detect able when it occupies more than 1.5-pixel sin a video image. This is the ultimate limit. One or two pixels can be easily confused with noise. In Fig.3, minimum smoke size versus detection range is shown for wild fire smoke using a visible range camera.

The curvature of the earth also affects the detection range. Forrangesabove20km, smoke should rise even higher to compensate for the earth's curvature. A sketch depicting a wildfire A smoke detection scenario from a camera placed on top of a 40-m-mast is presented in Fig. 4. At a

Distance of 40 km, a 40m $40 \times$ msmoke has to rise an additional 20 m to be detected by the camera on topofthemast.

The second criterion defines recognition which means that it is possible to make the distinction between a person, a car, a truck or wild fire. To store cognize an object it needs to occupy at least 6 pixels across its critical dimension in a video image. The third criterion defines identification. This term relates to military terminology. The critical dimension of the object should beat least 12 pixels so that the object is identified as "friend or foe". We can use Johnson's identification cr

Erion for wild fire identification be cause the white smoke may be due to a dirt cloud from an offroad vehicle or may be a cloud or it may be fog rising above the trees.

These criteria applied to IR-camera-based wildfire flame detection are summarized in the following figure. In Fig. 5, minimum flame sizes versus varying line-of-sight ranges are shown for de tection, recognition, and identification using an MWIR In P camera with an aspectralrangeof 3–5μm. Note that, a minimum flame size of $1m^2$ is enough to identify a wild fire range of 1.8km and it isenough to recognize it at a range of 2.7 km. However, at a distance of 11km, one can only detect the same fire.
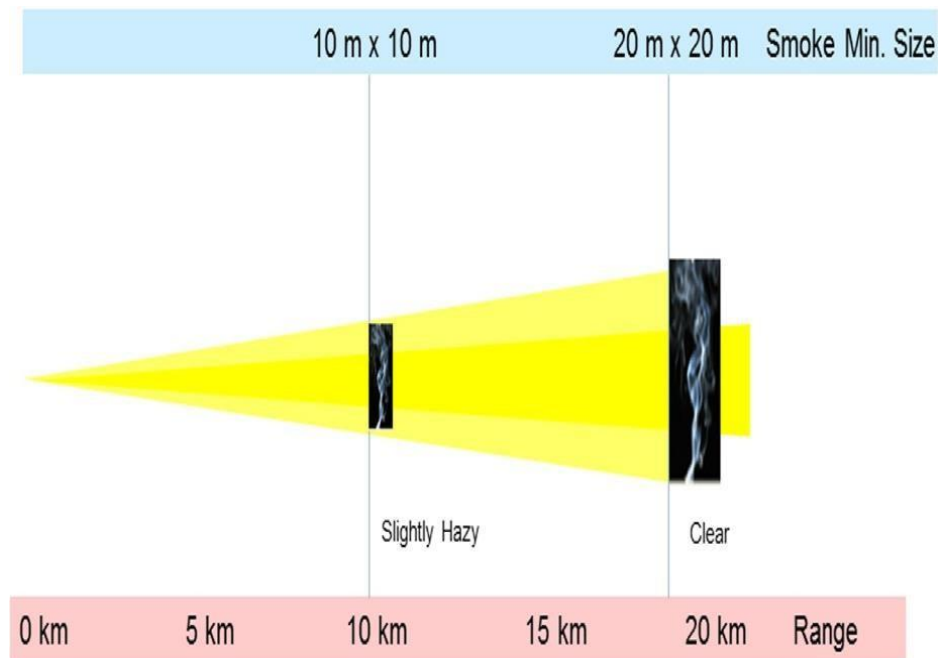
Fig.3. Minimum smoke size versus detection distance with a visible range camera.
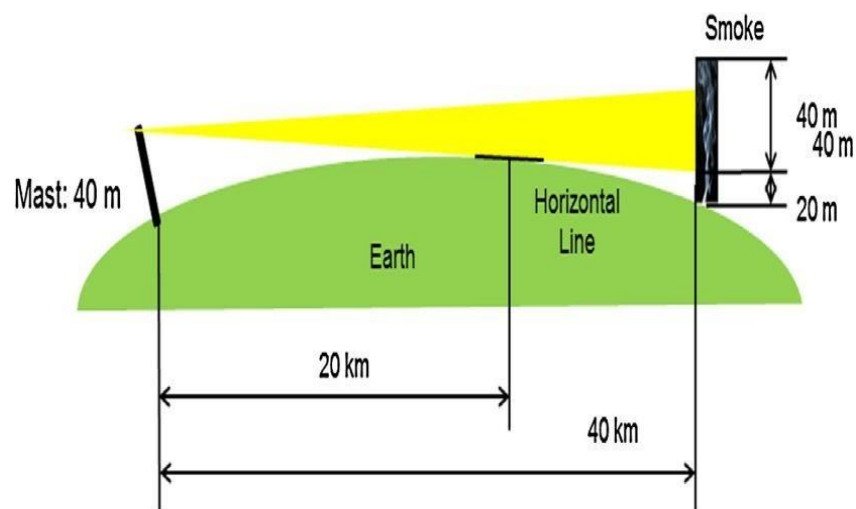
Fig.4. Effectoftheearth'scurvatureonwildfiresmokedetectionrange.
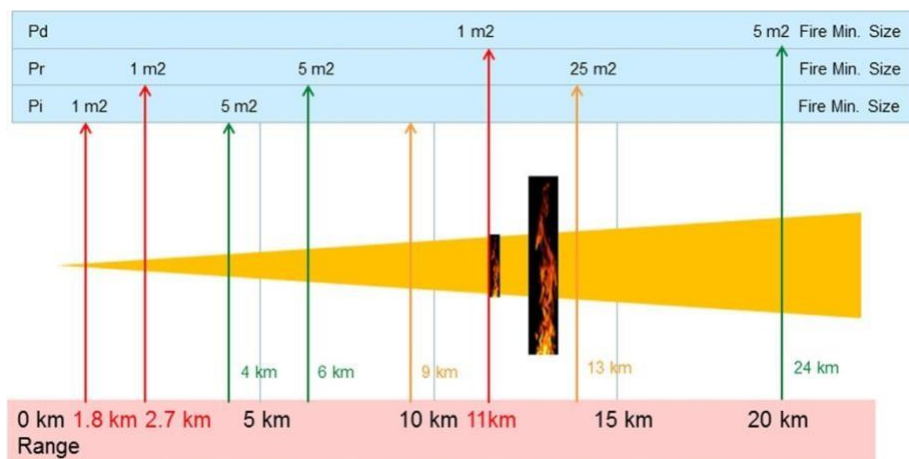
Fig.5. Minimum fire sizes versus detection, recognition and identification ranges.

4.4.1 Classification of Fire Pixel:

This section covers the detail of the proposed fire pixel classification algorithm. Figure 2 shows the flow chart of the proposed algorithm. Rule-based color model approach has been followed due to its simplicity and effectiveness. For that, color space RGB and YC_bC_r is chosen. For the classification of a pixel to be fire wehave identified seven rules. If a pixel satisfies these seven rules, we say that pixel belongs to the fire class.

A digitally colored image has three planes: Red, Green, and Blue (R, G, and B). The combination of RGB color planes gives the ability to devices to represent a color in the digital environment. Each color plane is quantized into discrete levels. Generally, 256 (8 bits per color plane) quantization level sure used for each plane, for instance, white is represented by (R, G, B) = (255, 255, 255), and black is represented by (R, G, B) = (0, 0, 0). A color image consists of pixels, where each pixel is represented by spatial location in the rectangular grid (x, y), and a color vector (R(x,y), G(x,y), B(x,y))corresponding to the spatial location(x,y).

A. Rule I

It can be noticed from figure 3 that for the fire regions, R channel has higher intensity values than the G channel, and the G channel has higher intensity values than the B channel.

To explain this idea better, we picked sample images from figure 5 (a) and segmented its fire pixels as shown in figure 4 (b) with green color. Then we calculate the mean values of R, G, and B planes in the segmented fire region so the original images. The results are given in Table I for the images given in figure 4. It is clear that, on average, the fire pixels show the characteristics that their R intensity value is greater

$$R_1(x,y) = \begin{cases} 1, \text{if } R(x,y) > G(x,y) > B(x,y) \\ 0, \text{otherwise} \end{cases}$$

------- (1)

Than G value and G intensity, value is greater than the B. So, for a pixel at a spatial location (x, y) to be a fire pixel the below rule must be satisfied.

Row index in Fig.7	Mean Y	Mean C_b	Mean C_r
1	130	106	153
2	189.3	48.1	158.2
3	195	65.8	155.6

Table: 4 Mean values of R, G, and B plane so fire regions for images given.

Fig.5: Flow chart of the proposed algorithm for forest fire detection.
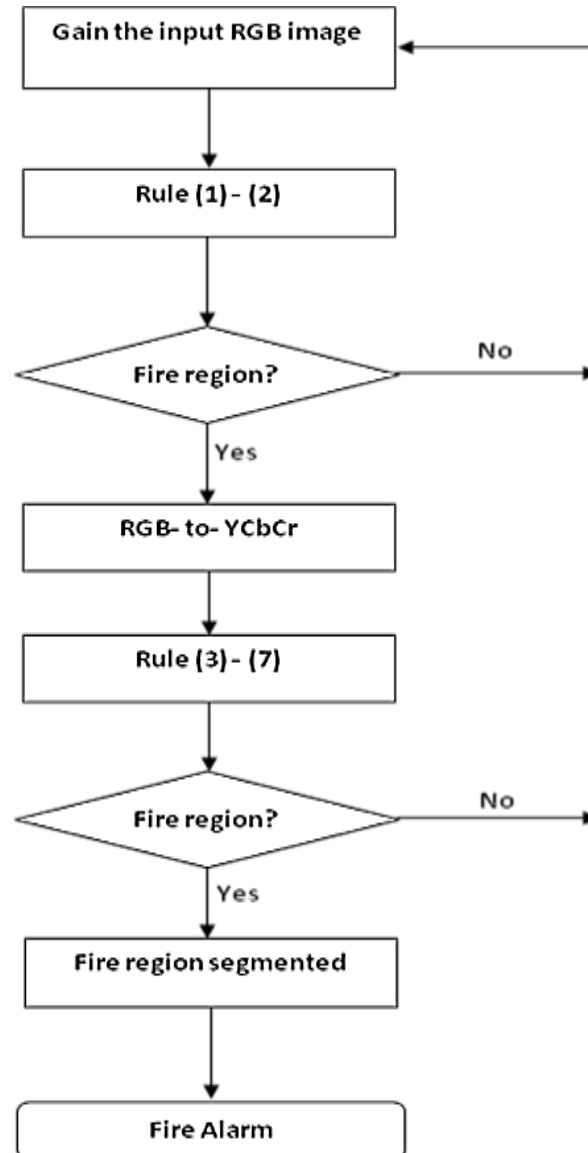
B. Rule II

$$R_2(x, y) = \begin{cases} 1, \text{if } (R(x, y) > 190) \cap (G(x, y) > 100) \cap (B(x, y) < 140 \\ 0, \text{otherwise} \end{cases}$$

------- (2)

Based on this observation of a large number of test images, the following rule can be established for detecting a fire pixel at the spatial location (x, y):

When the image is converted from RGB to YCbCr color space, intensity, and chrominance are easily discriminated. This help to model the fire region easily in YCbCr color space. The mean values of the three components Y, Cb, and Cr, denoted by Y mean, Cb mean and Cr mean respectively are computed as follows:

$$\begin{bmatrix} Y \\ Cb \\ Cr \end{bmatrix} = \begin{bmatrix} 0.2568 & 0.5041 & 0.0979 \\ -0.1482 & -0.2910 & 0.4392 \\ 0.4392 & -0.3678 & -0.0714 \end{bmatrix} \begin{bmatrix} R \\ G \\ B \end{bmatrix} + \begin{bmatrix} 16 \\ 128 \\ 128 \end{bmatrix}$$

------ (a)

where, (x,y) denotes the spatial location of pixels, M ×
Nisthetotalnumberofpixelsinthegivenimage

$$Y_{mean}(x, y) = \frac{1}{M \times N} \sum_{x=1}^{M} \sum_{y=1}^{N} Y(x, y)$$

$$Cb_{mean}(x, y) = \frac{1}{M \times N} \sum_{x=1}^{M} \sum_{y=1}^{N} Cb(x, y)$$

$$Cr_{mean}(x, y) = \frac{1}{M \times N} \sum_{x=1}^{M} \sum_{y=1}^{N} Cr(x, y)$$

----- (b)

Rules III and IV
From Table II, we have developed the following two rules. The rules were observed for a large number of test images from our data base.
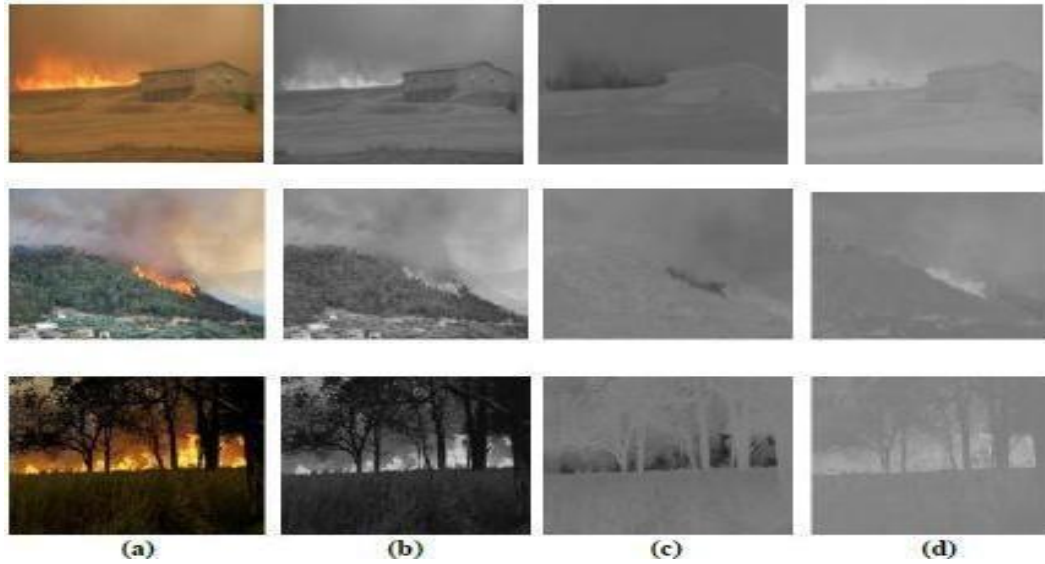
Fig.5: Original RGB image [19] in column [19](a), and Y, C_b, and C_r channels in column (b)-

The two rules for detecting a fire pixel at spatial location (x,y):

$$R_3(x,y) = \begin{cases} 1, \text{if } Y(x,y) \geq Cb(x,y) \\ 0, \text{otherwise} \end{cases}$$

----- (3)

$$R_4(x,y) = \begin{cases} 1, \text{if } Cr(x,y) \geq Cb(x,y) \\ 0, \text{otherwise} \end{cases}$$

------ (4)

Rule V

The flame region is generally the brightest in the observed scene, the mean values of the three channels, in the overall image Ymean, Cbmean, and Crmean contain valuable information. From figure 7, it can be observed that for the flame region, the value of the Y component is bigger than the mean Y component of the overall image while the value of the Cb component is in general smaller than the mean Cb value of the overall image. Furthermore, the Cr component of the flame region is bigger than the mean Cr component.

These observations which are verified over countless experiments with images containing fire regions are formulated as the following rule:

$$R_5(x, y) = \begin{cases} 1, \text{if } (Y(x, y) \geq Y_{mean}(x, y)) \cap (Cb(x, y) \leq Cb_{mean}(x, y)) \\ \quad \cap (Cr(x, y) \geq Cr_{mean}(x, y)) \\ \\ 0, \text{otherwise} \end{cases} \quad \text{------------- (5)}$$

where, R5(x,y) indicates that any pixel that satisfies the condition given in eq.(5) is considered to be fire pixel.

Rule VI

It can easily be observed from Figure 7(c) and Figure 7(d) that there is a significant difference between the Cb and Cr components of the fire pixels. For the fire pixel, the Cb component is predominantly "black" (lower intensity) while the Cr component, on the other hand, is predominantly "white" (higher intensity).
This fact can be translated into another rule as follows:

$$R_6(x, y) = \begin{cases} 1, \text{if } |Cb(x, y) - Cr(x, y)| \geq Th \\ 0, \text{otherwise} \end{cases} \quad \text{---- (6)}$$

where the value of Th is accurately determined according to a Receiver Operating Characteristics (ROC) Curve[14].
The ROC curve is obtained by experimenting with different values of Th (ranging from 1 to 100) over 100 color images. First, the fire-pixel regions are manually segmented from each color image. Therules 1 through 5 (at a chosen value of Th) are then applied to the manually-segmented fire regions. The true positive is defined as the decision when an image contains a fire, and the false positive is defined as the decision when an image contains no fire but is classified as having fire. The ROC curve consists of 100 data points corresponding to different Th values, the corresponding true positive (i.e., correct-detection) and false positive (i.e., false-alarm) rates arecomputed and recorded.
The correct detection is defined as the same decision when an image indeed contains a fire incident, while the false alarm is defined as an incorrect decision when an image contains no fire but is mis-detected as having fire. For good fire detection system, it should not miss any fire alarms, with

the established ROC curve, the value of Th is picked such that the systems true positive rate is high enough.

Fig.9: (a) Original RGB image [19], (b) RGB-to-YCbCr converted image, and(c) corresponding fire region manually labeled with green color on YCbCr image.

Based on this observation of a large number of test images, the following rule can beestablished for detecting a fire pixel at the spatial location (x,y):

$$R_7(x,y) = \begin{cases} 1, \text{if } (Cb(x,y) \leq 120) \cap (Cr(x,y) \geq 150) \\ 0, \text{otherwise} \end{cases} \quad \text{--- (7)}$$

A pixel is classified to fire class if all the *Rules I-VII* is satisfied by that pixel. The process of segmentation can be easily understood with the help of figure 11 which explains step-by-step manner. As can be seen from figure 11 each rule alone will produce a false alarm, but their overall combination produces the result in finding out the fire region in the corresponding image. Figure 12 shows the experimental results for different input images.

Conclusion & Discussion: Furthermore, to explore the evolution of the forest fire detection research domain, we carried out abibliometric analysis. The initial search yielded over 2024 papers related to forest fire detect published in the Web of Science (WoS) database. Figure **6** shows the trend in the number of articles published between 1 January 1990 and 31 October 2020. Narrowing the results to only the imaging research area, the search yielded 697 published articles (Figure 6). These results show that there is a growth in publications in the last 30 years. Of these, 378

are related to forest fire detection based on terrestrial systems, 59 based on aerial systems, and 260 based on satellite systems (Figure 7). The results of Figure 7 indicate that the field of forest fire detection in the image research area for terrestrial, aerial, and satellite- based systems is still evolving.

During the last two decades, video fire detection research led to commercial and experimental VFD systems. They are especially used in high-risk building sand areas. Hundreds of video smoke detection systems are installed in look out to sand poles for wild fire detection. Although they are not fully automated systems they are invaluable tools for security personal. Whenever the VFD system produces an alarm, the operator can check if it is a real fire or a false alarm. In this way, the operator can handle multiple cameras.

We believe that further search Swill prove the detection per-romance of the VFD systems while reducing the false alarm rates. We also believe that multi-modal systems employing IR and regular cameras will provide fully reliable VFD solutions. Such systems are currently expensive, but they will be feasible with the decline of IR camera costs shortly.
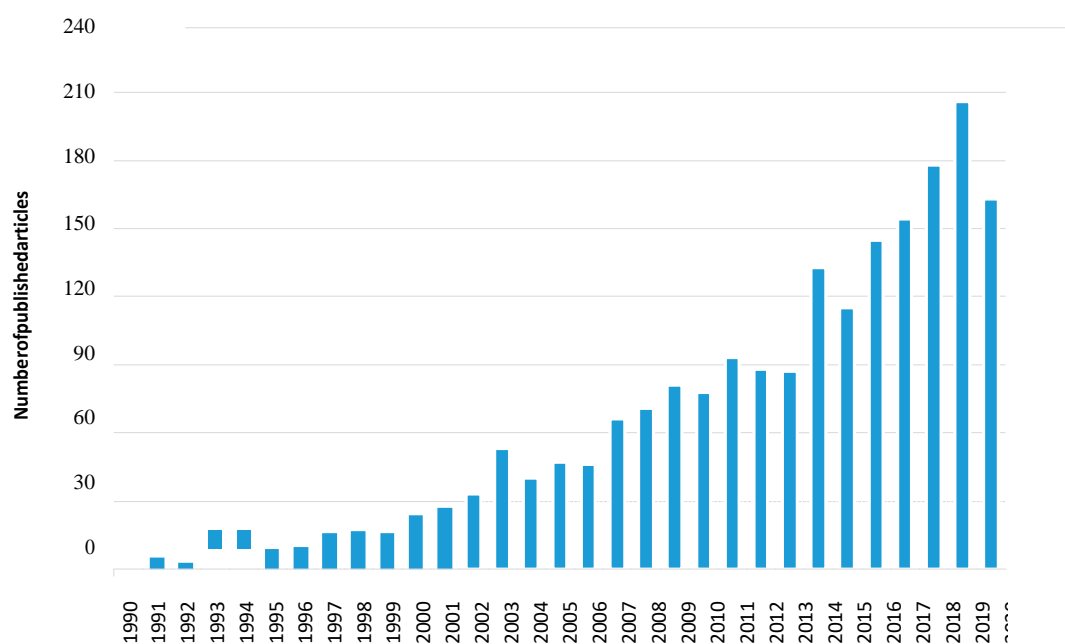
Figure5. The number of published articles per year related to forest fire detection. Data are from Web of Science [127]fordatesbetween1990toOctober2020.
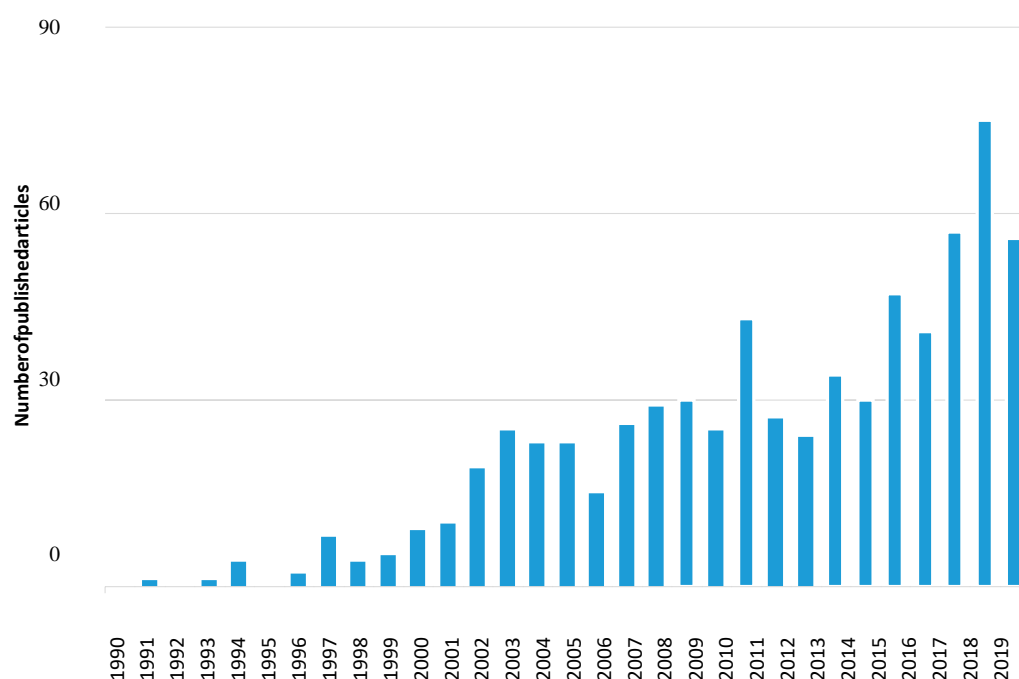

Figure6. The number of published articles per year related to forest fire detection in the imaging research area. Data are Web of Science[127]fordatesbetween1990toOctober2020.

References

1. Tanase, M.A.; Aponte, C.; Mermoz, S.; Bouvet, A.; Le Toan, T.; Heurich, M. Detection of windthrows andinsectoutbreaksbyL-bandSAR:AcasestudyintheBavarianForestNationalPark.*RemoteSens.Environ.***2018**,*209*,700–711.[CrossRef]

2. Pradhan, B.; Suliman, M.D.H.B.; Awang, M.A.B. Forest fire susceptibility a nd risk mapping using remotesensingandgeographicalinformationsystems(GIS).*DisasterPrev.Manag.Int.J.***2007**,*16*.[CrossRef]

3. Kresek, R. History of the Osborne Firefinder.2007.Available online:http://nysforestrangers.com/archives/osborne%20firefinder%20by%20kresek.pdf(accessedon7September2020).

4. Bouabdellah,K.;Noureddine,H.;Larbi,S.Usingwirelesssensornetworksforreliableforestfiresdetection. *ProcediaComput.Sci.***2013**,*19*,794–801.[CrossRef]

5. Gaur,A.;Singh,A.;Kumar,A.;Kulkarni,K.S.:Lala,S.;Kapoor,K.;Srivastava,V.;Kumar,A.; Mukhopadhyay,S.C.Firesensingtechnologies:Areview.*IEEESens.J.***2019**,*19*,3191–3202.[CrossRef]

6. Gaur, A.; Singh, A.; Kumar, A.; Kumar, A.; Kapoor, K. Video Flame and Smoke Based Fire DetectionAlgorithms:ALiteratureReview.*FireTechnol.***2020**,*56*,1943–1980.[CrossRef]

7. Kaabi,R.;Frizzi,S.;Bouchouicha,M.;Fnaiech,F.;Moreau,E.Videosmokedetectionreview:StateoftheartofsmokedetectionininvisibleandIRrange.InProceedingsofthe2017InternationalConferenceonSmart,MonitoredandControlledCities(SM2C),Kerkennah-Sfax,Tunisia,17February2017;pp.81–86.

8. Garg,S.;Verma,A.A.ReviewSurveyonSmokeDetection.*Imp.J.Interdiscip.Res.***2016**,*2*,935–939.

9. Memane, S.E.; Kulkarni, V.S. A review on flame and smoke detection techniques in video's.*Int. J. Adv. Res.Electr.Electr.Instrum.Eng.***2015**,*4*,885–889.

10. Bu,F.;Gharajeh,M.S.Intelligentandvision-basedfiredetectionsystems:Asurvey.*ImageVis.Comput.***2019**, *91*,103803.[CrossRef]

11. Yuan, C.; Zhang, Y.; Liu, Z. A survey on technologies for automatic forest fire monitoring, detection, andfighting using unmanned aerial vehicles and remote sensing techniques. *Can. J. For. Res.* **2015**, *45*, 783–792.[CrossRef]

12. Allison,R.S.;Johnston,J.M.;Craig,G.;Jennings,S.Airborneopticalandthermalremotesensingforwildfiredetectionand monitoring.*Sensors***2016**,*16*,1310.[CrossRef]

13. Nixon,M.;Aguado,A.*FeatureExtractionandImageProcessingforComputerVision*;AcademicPress:Cambridge , MA,USA,2019.

14. Mather,P.;Tso,B.*ClassificationMethodsforRemotelySensedData*;CRCPress:BocaRaton,FL,USA,2016.

15. Çetin,A.E.;Dimitropoulos,K.;Gouverneur,B.;Grammalidis,N.;Günay,O.;Habiboğlu,Y.H.;Töreyin,B. U.; Verstockt,S.Videofiredetection–review.*Dig.SignalProcess.***2013**,*23*,1827–1843.[CrossRef]

16. Töreyin,B.U.;Cinbis, R.G.; Dedeoglu, Y.; Cetin, A.E. Fire detectionininfrared video using wavelet analysis. *Opt.Eng.***2007**,*46*,067204.[CrossRef]

17. Cappellini, Y.; Mattii, L.; Mecocci, A. An Intelligent System for Automatic Fire Detection in Forests.In *RecentIssuesin PatternAnalysis andRecognition*;Springer:Berlin/Heidelberg,Germany,1989;pp.563–570.

18. Chen,T.H.;Wu,P.H.;Chiou,Y.C.Anearlyfire-detectionmethodbasedonimageprocessing.InProceedingsofthe2004InternationalConferenceonImageProcessing(ICIP04),Singapore,24–27October2004;Volume3,pp.1707–1710.

19. Dimitropoulos,K.;Gunay,O.;Kose,K.;Erden, F.; Chaabene, F.; Tsalakanidou, F.; Grammalidis, N.;Çetin,E.Flamedetection for video-based early fire warning for the protection of cultural heritage.In Proceedings of the Euro-Mediterranean Conference, Limassol, Cyprus, 29 October–3 November 2012;Springer:Berlin/Heidelberg,Germany;pp.378–387.

20. Celik,T.;Demirel,H.Firedetectioninvideosequencesusingagenericcolormodel.*FireSaf.J.***2009**,*44*, 147–158.[CrossRef]

21. Celik, T. Fast and efficient method for fire detection using image processing.*ETRI J.* **2010**, *32*, 881–890.[CrossRef]

22. Marbach,G.;Loepfe,M.;Brupbacher,T.Animageprocessingtechniqueforfiredetectioninvideoimages. *FireSaf.J.***2006**,*41*,285–289.[CrossRef]

23. Kim, D.; Wang, Y.F. Smoke detection in video. In Proceedings of the 2009 WRI World Congress on ComputerScienceandInformationEngineering,LosAngeles,CA,USA,31March–2April2009;Volume5,pp.759–763.

24. Yamagishi, H.; Yamaguchi, J. Fire flame detection algorithm using a color camera.In Proceedings of theMHS'99, 1999 International Symposium on Micromechatronics and Human Science (Cat. No. 99TH8478),Nagoya,Japan,23 – 26November1999;pp.255–260.

25. Dimitropoulos,K.;Tsalakanidou,F.;Grammalidis,N.Flamedetectionforvideo-basedearlyfirewarningsystemsand3Dvisualizationoffirepropagation.InProceedingsofthe13thIASTEDInternationalConference on Computer Graphics and Imaging (CGIM 2012), Crete, Greece, 18–20 June 2012.Availableonline:https://zenodo.org/record/1218#.X6qSVmj7Sbg(accessedon10November2020).

26. *Zhang,Z.;Shen,T.;Zou,J.Animprovedprobabilisticapproachforfiredetectioninvideos.* *FireTechnol.* **2014**, *50*, 745–752.[CrossRef]

27. Avgerinakis, K.; Briassouli, A.; Kompatsiaris, I. Smoke detection using temporal HOGHOF descriptors andenergy colour statistics from video. In Proceedings of the International Workshop on Multi-Sensor SystemsandNetworks forFire Detectionand Management,Antalya, Turkey,8–9 November2012.

28. Mueller,M.;Karasev,P.;Kolesov,I.;Tannenbaum,A.Opticalflowestimationforflamedetectioninvideos. *IEEETrans.ImageProcess.***2013**,*22*,2786–2797.[CrossRef]

29. *Chamberlin,D.S.;Rose,A.TheFirstSymposium(International)onCombustion.* *Combust.Inst.Pittsburgh* **1965**,*1965*,27–32.

30. Günay,O.;Taşdemir,K.;Töreyin,B.U.;Çetin,A.E.FiredetectioninvideousingLMSbasedactivelearning. *FireTechnol.***2010**,*46*,551–577.[CrossRef]

31. *Teng,Z.;Kim,J.H.;Kang,D.J.FiredetectionbasedonhiddenMarkovmodels.Int.J.ControlAutom.Syst.* **2010**, *8*, 822–830.[CrossRef]

32. Töreyin,B.U.Smokedetectionincompressedvideo.In*ApplicationsofDigitalImageProcessingXLI*;InternationalSocietyforOpticsandPhotonics:Bellingham,WA,USA,2018;Volume10752,p.1075232.

33. Savcı,M.M.;Yıldırım,Y.;Saygılı,G.;Töreyin,B.U.FiredetectioninH.264compressedvideo.InProceedingsof the ICASSP 2019– 2019 IEEE International Conference on Acoustics, Speech and Signal Processing (ICASSP),Brighton,UK,12–17May2019;pp.8310–8314.

34. Chen,J.;He,Y.;Wang,J.Multi-featurefusionbasedfastvideoflamedetection.*Build.Environ.***2010**,*45*, 1113–1122.[CrossRef]

35. Töreyin,B.U.;Dedeoğlu,Y.;Güdükbay,U.;Cetin,A.E.Computervisionbasedmethodforreal-timefireand flame detection.*PatternRecognit.Lett.***2006**,*27*, 49–58.[CrossRef]

36. Barmpoutis, P.; Dimitropoulos, K.; Grammalidis, N. Real time video fire detection using spatio-temporalconsistency energy. In Proceedings of the 10th IEEE International Conference on Advanced Video and SignalBased Surveillance, Krakow, Poland, 27–30 August2013; pp. 365–370.

37. Arrue, B.C.; Ollero, A.; De Dios, J.M. An intelligent system for false alarm reduction in infrar ed forest-firedetection.*IEEEIntell.Syst.TheirAppl.***2000**, *15*,64–73.[CrossRef]

38. Grammalidis,N.;Cetin,E.;Dimitropoulos,K.;Tsalakanidou,F.;Kose,K.;Gunay,O.;Gouverneur,B.;Torri,D.;Kuruoglu,E.;Tozzi,S.;etal.AMulti-SensorNetworkfortheProtectionofCulturalHeritage.InProceedingsofthe19thEuropeanSignalProcessingConference,Barcelona,Spain,29August–2September2011.

39. Bosch, I.; Serrano, A.; Vergara, L. Multisensor network system for wildfire detection using infrared imageprocessing.*Sci.WorldJ.***2013**,*2013*,402196.[CrossRef]

40. Barmpoutis,P.;Dimitropoulos,K.;Grammalidis,N.Smokedetectionusingspatio-temporalanalysis,motionmodelinganddynamictexturerecognition.InProceedingsofthe22ndEuropeanSignalProcessingConference,Lisbon, Portugal, 1–5 September 2014; pp. 1078–1082.

41. Dimitropoulos, K.; Barmpoutis, P.; Grammalidis, N. Spatio-temporal flame modeling and dynamic textureanalysis for automatic video-based fire detection. *IEEE Trans. Circuits Syst. Video Technol.* **2015**, *25*, 339–351.[CrossRef]

42. Prema, C.E.; Vinsley, S.S.; Suresh, S. Efficient flame detection based on static and dynamic texture analysis inforest fire detection.*FireTechnol.***2018**, *54*, 255–288.[CrossRef]

43. Dimitropoulos, K.; Barmpoutis, P.; Grammalidis, N. Higher order linear dynamical systems for smokedetection invideo surveillance applications.*IEEE Trans. Circuits Syst. Video Technol.* **2016**, *27*, 1143–1154.[CrossRef]

44. Dimitropoulos,K.;Barmpoutis,P.;Kitsikidis,A.;Grammalidis,N.Classificationofmultidimensionaltime-evolving data using histograms of grassmannian points. *IEEE Trans. Circuits Syst. Video Technol.* **2016**,*28*,892–905.[CrossRef]

45. Schmidhuber,J.Deeplearninginneuralnetworks:Anoverview.*NeuralNetw.***2015**,*61*,85–117.[CrossRef]

46. Krizhevsky,A.;Sutskever,I.;Hinton,G.E.Imagenetclassificationwithdeepconvolutionalneuralnetworks. In*AdvancesinNeuralInformationProcessingSystems*;MITPress:Cambridge,MA,USA,2012;pp.1097–1105.

47. Luo, Y.; Zhao, L.; Liu, P.; Huang, D. Fire smoke detection algorithm based on motion characteristic andconvolutionalneuralnetworks.*Multimed.ToolsAppl.***2018**,*77*,15075–15092.[CrossRef]

48. Zhao, L.; Luo, Y.M.; Luo, X.Y. Based on dynamic background update and dark channel prior of fire smokedetection algorithm.*Appl.Res.Comput.***2017**,*34*,957–960.

49. Wu,X.;Lu,X.;Leung,H.Anadaptivethresholddeeplearningmethodforfireandsmokedetection.In Proceedings of the 2017 IEEE International Conference on Systems,Man,and Cybernetics (SMC),Banff,AB,Canada,5– 8October2017;pp.1954–1959.

50. Sharma, J.; Granmo, O.C.; Goodwin, M.; Fidje, J.T. Deep convolutional neural networks for fire detection inimages. In Proceedings of the International Conference on Engineering Applications of Neural Networks,Athens,Greece,25–27August2017;Springer:Berlin/Heidelberg,Germany,2017;pp.183–193.

51. Zhang,Q.;Xu,J.;Xu,L.;Guo,H.Deepconvolutionalneuralnetworksforforestfiredetection.In *2016 InternationalForumonManagement,EducationandInformationTechnologyApplication*;AtlantisPress:Paris,France,2016.

52. Muhammad, K.; Ahmad, J.; Mehmood, I.; Rho, S.; Baik, S.W. Convolutional neural networks based firedetectioninsurveillancevideos.*IEEEAccess***2018**,*6*,18174–18183.[CrossRef]

53. Shen, D.;Chen, X.;Nguyen, M.; Yan, W.Q. Flame detection using deep learning. In Proceedings of the20184thInternationalConferenceonControl,AutomationandRobotics(ICCAR),Auckland,NewZealand,20–23April2018;pp.416–420.

54. Frizzi, S.; Kaabi, R.; Bouchouicha, M.; Ginoux, J.M.; Moreau, E.; Fnaiech, F. Convolutional neural network for video fire and smoke detection. In Proceedings of the IECON 2016-42nd Annual Conference of the IEEEIndustrialElectronicsSociety,Florence,Italy,23–26October2016;pp.877–882.

55. Muhammad,K.;Ahmad,J.;Lv,Z.;Bellavista,P.;Yang,P.;Baik,S.W.EfficientdeepCNN-basedfiredetectionand localization in video surveillance applications. *IEEE Trans. Syst. Man Cybern. Syst.* **2018**, *49*, 1419–1434.[CrossRef]

56. Muhammad, K.; Ahmad, J.; Baik, S.W. Early fire detection using convolutional neural networks duringsurveillanceforeffectivedisastermanagement.*Neurocomputing***2018**,*288*,30–42.[CrossRef]

57. Dunnings, A.J.; Breckon, T.P. Experimentally defined convolutional neural network architecture variants fornon-temporal real-time fire detection.In Proceedings of the 2018 25th IEEE International Conference onImageProcessing(ICIP),Athens,Greece,7–10October2018;pp.1558–1562.

58. Sousa,M.J.;Moutinho,A.;Almeida,M.Wildfiredetectionusingtransferlearningonaugmenteddatasets. *ExpertSyst.Appl.***2020**,*142*,112975.[CrossRef]

59. Toulouse,T.;Rossi,L.;Campana,A.; Celik, T.; Akhloufi, M.A. Computer vision for wildfire research:Anevolvingimagedatasetforprocessingandanalysis.*FireSaf.J.***2017**,*92*,188–194.[CrossRef]

60. Barmpoutis, P.; Dimitropoulos, K.; Kaza, K.; Grammalidis, N. Fire Detection from Images Using FasterR-CNN and Multidimensional Texture Analysis. In Proceedings of the ICASSP 2019–2019 IEEE InternationalConferenceonAcoustics,SpeechandSignalProcessing,Brighton,UK,12–17May2019;pp.8301–8305.

61. Lin,G.;Zhang,Y.;Xu,G.;Zhang,Q.Smokedetectiononvideosequencesusing3Dconvolutionalneuralnetworks.*FireTech nol.***2019**,*55*,1827–1847.[CrossRef]

62. Jadon,A.;Omama,M.;Varshney,A.;Ansari,M.S.;Sharma,R.Firenet:Aspecializedlightweightfire&smokedetectionmod elforreal-timeiotapplications.*arXiv***2019**,arXiv:1905.11922.

63. Zhang,Q.X.;Lin,G.H.;Zhang,Y.M.;Xu,G.;Wang,J.J.WildlandforestfiresmokedetectionbasedonfasterR -CNN using synthetic smoke images.*ProcediaEng.***2018**, *211*, 441–446.[CrossRef]

64. Kim,B.;Lee,J.Avideo-basedfiredetectionusingdeeplearningmodels.*Appl.Sci.***2019**,*9*,2862.[CrossRef]

65. Shi, L.; Long, F.; Lin, C.; Zhao, Y. Video-based fire detection with saliency detection and convolutional neuralnetworks.In*InternationalSymposiumonNeuralNetworks*;Springer:Cham,Switzerland,2017;pp.299–309.

66. Wang, K.;Lin, L.;Lu, J.;Li, C.;Shi, K. PISA: Pixelwise image saliency by aggregating complementaryappearance contrast measures with edge-preserving coherence.*IEEE Trans.Image Process.***2015**, *9*, 2115–2122.[CrossRef][PubMed]

67. Yuan, F.; Zhang, L.; Xia, X.; Wan, B.; Huang, Q.; Li, X. Deep smoke segmentation. *Neurocomputing* **2019**, *357*,248–260.[CrossRef]

68. Cheng, S.;Ma, J.;Zhang, S. Smoke detection and trend prediction method based on Deeplabv3+ andgenerativeadversarialnetwork.*J.Electron.Imaging***2019**,*28*,033006.[CrossRef]

69. Aslan, S.; Güdükbay, U.; Töreyin, B.U.; Çetin, A.E. Early wildfire smoke detection based on motion-basedgeometric image transformation and deep convolutional generative adversarial networks. In Proceedings ofthe ICASSP 2019–2019 IEEE International Conference on Acoustics, Speech and Signal Processing (ICASSP),Brighton,UK,12–17May2019;pp.8315–8319.

70. Hristov, G.; Raychev, J.; Kinaneva, D.; Zahariev, P. Emerging methods for early detection of forest fires usingunmanned aerial vehicles and lorawan sensor networks. In Proceedings of the IEEE 28th EAEEIE AnnualConference, Hafnarfjordur, Iceland, 26–28September 2018; pp.1–9.

71. Stearns, J.R.; Zahniser, M.S.; Kolb, C.E.; Sandford, B.P. Airborne infrared observations and analyses of a largeforestfire.*Appl.Opt.***1986**,*25*,2554–2562.[CrossRef][PubMed]

72. DenBreejen,E.;Breuers,M.;Cremer,F.;Kemp,R.;Roos,M.;Schutte,K.;DeVries,J.S. AutonomousForest Fire Detection; ADAI-Associacao para o Desenvolvimento da Aerodinamica Industrial: Coimbra, Portugal,1998;pp.2003–2012.

73. Yuan,C.;Liu,Z.;Zhang,Y.UAV-basedforestfiredetectionandtrackingusingimageprocessingtechniques.InProceedingsofthe2015InternationalConfere nceonUnmannedAircraftSystems(ICUAS),Denver,CO,USA,9–12June2015;pp.639–643.

74. Yuan,C.;Liu,Z.;Zhang,Y.Learning-basedsmokedetectionforunmannedaerialvehiclesappliedtoforestfire surveillance.*J.Intell.Robot.Syst.***2019**, *93*, 337–349.[CrossRef]

75. Dang-Ngoc, H.; Nguyen-Trung, H. Aerial Forest Fire Surveillance-Evaluation of Forest Fire Detection Modelusing Aerial Videos.In Proceedings of the 2019 International Conference on Advanced Technologies forCommunications(ATC),Hanoi,Vietnam,17–19October2019;pp.142–148.

76. Yuan, C.; Liu, Z.; Zhang, Y. Aerial images-based forest fire detection for firefighting using optical remotesensingtechniquesandunmannedaerialvehicles.*J.Intell.Robot.Syst.***2017**,*88*,635–654.[CrossRef]

77. DeSousa,J.V.R.;Gamboa,P.V.AerialForestFireDetectionandMonitoringUsingaSmallUAV. KnEEng. **2020**,242–256.[CrossRef]

78. Esfahlani,S.S.Mixedrealityandremote sensingapplicationofunmannedaerial vehicleinfireandsmokedetection.*J.Ind.Inf.Integr.***2019**,*15*,42–49.[CrossRef]

79. Sudhakar,S.;Vijayakumar,V.;Kumar, C.S.; Priya, V.; Ravi, L.; Subramaniyaswamy, V. UnmannedAerial Vehicle (UAV) based Forest Fire Detection and monitoring for reducing false alarms in forest- fires.*Comput.Commun.***2020**,*149*,1–16.[CrossRef]

80. Kinaneva,D.;Hristov,G.;Raychev,J.;Zahariev,P.Earlyforestfiredetectionusingdronesandartificialintelligence. In

Proceedings of the 2019 42nd International Convention on Information and CommunicationTechnology,ElectronicsandMicroelectronics(MIPRO),Opatija,Croatia,20–24May2019;pp.1060–1065.

81. Chen, Y.; Zhang, Y.; Xin, J.; Yi, Y.; Liu, D.; Liu, H. A UAV-based Forest Fire Detection Algorithm UsingConvolutional Neural Network.In Proceedings of the IEEE 37th Chinese Control Conference, Wuhan, China,25–27July2018;pp.10305–10310.

82. Merino, L.; Caballero, F.; Martínez-De-Dios, J.R.; Maza, I.; Ollero, A. An unmanned aircraft system forautomaticforestfiremonitoringandmeasurement.*J.Intell.Robot.Syst.***2012**,*65*,533–548.[CrossRef]

83. Zhao, Y.; Ma, J.; Li, X.; Zhang, J. Saliency detection and deep learning -based wildfire identification in UAVimagery.*Sensors***2018**,*18*,712.[CrossRef][PubMed]

84. Tang, Z.; Liu, X.; Chen, H.; Hupy, J.; Yang, B. Deep Learning Based Wildfire Event Object Detection from 4KAerialImagesAcquiredbyUAS.*AI* **2020**,*1*,166–179.[CrossRef]

85. Jiao, Z.; Zhang, Y.; Mu, L.; Xin, J.; Jiao, S.; Liu, H.; Liu, D. A YOLOv3-based Learning Strategy for Real-timeUAV-based Forest Fire Detection.In Proceedings of the 2020 Chinese Control and Decision Conference(CCDC),Hefei,China,22– 24August2020;pp.4963–4967.

86. Jiao, Z.; Zhang, Y.; Xin, J.; Mu, L.; Yi, Y.; Liu, H.; Liu, D. A Deep Learning Based Forest Fire DetectionApproach Using UAV and YOLOv3. In Proceedings of the 2019 1st International Conference on IndustrialArtificialIntelligence(IAI),Shenyang,China,23–27July2019;pp.1–5.

87. Srinivas,K.;Dua,M.FogComputingandDeepCNNBasedEfficientApproachtoEarlyForestFireDetectionwithUnmanned AerialVehicles.InProceedingsoftheInternationalConferenceonInventiveComputationTechnologies,Coimbatore,India,29–30August2019;Springer:Cham,Switzerland,2020;pp.646–652.

88. Barmpoutis, P.; Stathaki, T. A Novel Framework for Early Fire Detection Using Terrestrial and Aerial360 -Degree Images. In Proceedings of the International Conference on Advanced Concepts for IntelligentVisionSystems,Auckland, NewZealand, 10–14February2020;Springer:Cham,Switzerland,2020;pp.63–74.

89. Barmpoutis, P.;Stathaki, T.;Dimitropoulos, K.;Grammalidis, N. Early Fire Detection Based on Aerial360-Degree Sensors, Deep Convolution Neural Networks and Exploitation of Fire Dynamic Textures. *RemoteSens.***2020**,*12*,3177.[CrossRef]

90. He, L.; Li, Z. Enhancement of a fire detection algorithm by eliminating solar reflection in the mid-IR band:Application to AVHRR data.*Int.J.RemoteSens.***2012**, *33*, 7047–7059.[CrossRef]

91. He, L.;Li, Z. Enhancement of fire detection algorithm by eliminating solar contamination effect andatmosphericpathradiance:ApplicationtoMODISdata.*Int.J.RemoteSens.***2011**,*32*,6273–6293.[CrossRef]

92. Csiszar, I.; Schroeder, W.; Giglio, L.; Ellicott, E.; Vadrevu, K.P.; Justice, C.O.; Wind, B. Active fires fromtheSuomiNPPVisibleInfraredImagingRadiometer,Suite:ProductStatusandfirstevaluationresults. *J.Geophys.Res.Atmos.***2014**,*119*,803–816.[CrossRef]

93. Schroeder, W.; Oliva, P.; Giglio, L.; Csiszar, I.A. The New VIIRS 375m Active Fire Detection Data Product:AlgorithmDescriptionandInitialAssessment.*RemoteSens.Environ.***2014**,*143*,85–96.[CrossRef]

94. Sayad,Y.O.;Mousannif,H.;AlMoatassime,H.Predictivemodelingofwildfires:Anewdatasetandmachinelearning approach.*FireSaf.J.***2019**,*104*,130–146.[CrossRef]

95. Shukla, B.P.; Pal, P.K. Automatic smoke detection using satellite imagery: Preparatory to smokedetectionfromInsat-3D.*Int.J.RemoteSens.***2009**,*30*,9–22.[CrossRef]

96. Li,X.;Song,W.;Lian,L.;Wei,X.Forestfiresmokedetectionusingback-propagationneuralnetworkbasedonMODISdata.*RemoteSens.***2015**,*7*,4473–4498.[CrossRef]

97. Li, Z.; Khananian, A.; Fraser, R.H.; Cihlar, J. Automatic detection of fire smoke using artificial neural networksandthresholdapproachesappliedtoAVHRRimagery.*IEEETrans.Geosci.Remote Sens.***2001**,*39*,1859–1870.

98. Hally,B.;Wallace,L.;Reinke,K.;Jones,S.;Skidmore,A.Advancesinactivefiredetectionusingamulti-temporal method for next-generation geostationary satellite data. *Int. J. Dig. Earth* **2019**, *12*, 1030–1045.[CrossRef]

99. Giglio, L.; Schroeder, W.; Justice, C.O. The Collection 6 MODIS Active Fire Detection Algorithm and FireProducts.*RemoteSens.Environ.***2016**,*178*,31–41.[CrossRef]

100. Wickramasinghe,C.;Wallace,L.;Reinke,K.;Jones,S.IntercomparisonofHimawari-8AHI-FSAwithMODISandVIIRSactivefireproducts.*Int.J.Dig.Earth***2018**.[CrossRef]

101. Lin, L.; Meng, Y.; Yue, A.; Yuan, Y.; Liu, X.; Chen, J.; Zhang, M.; Chen, J. A spatio-temporal model for forestfiredetectionusingHJ-IRSsatellitedata.*RemoteSens.***2016**,*8*,403.[CrossRef]

102. Ba, R.; Chen, C.; Yuan, J.; Song, W.; Lo, S. SmokeNet: Satellite smoke scene detection using convolutionalneuralnetworkwithspatialandchannel-wiseattention.*RemoteSens.***2019**,*11*,1702.[CrossRef]

103. Vani, K. Deep Learning Based Forest Fire Classification and Detection in Satellite Images.In Proceedings ofthe 2019 11th International Conference on Advanced Computing (ICoAC), Chennai, India, 18–20 December2019;pp.61–65.

104. Hally, B.; Wallace, L.; Reinke, K.; Jones, S. A Broad-Area Method for the Diurnal Characterisation of UpwellingMediumWaveInfraredRadiation.*RemoteSens.***2017**,*9*,167.[CrossRef]

105. Fatkhuroyan, T.W.; Andersen, P. Forest fires detection in Indonesia using satellite Himawari-8 (case study:Sumatera and Kalimantan on august-october 2015). In *IOP Conference Series: Earth and Environmental Science*;IOPPublishingLtd.:Bristol,UK,2017;Volume54,pp.1315–1755.

106. Xu, G.;Zhong, X. Real-time wildfire detection and tracking in Australia using geostationary satellite:Himawari-8.*RemoteSens.Lett.***2017**, *8*,1052–1061.[CrossRef]

107. Xie, Z.; Song, W.; Ba, R.; Li, X.; Xia, L. A spatiotemporal contextual model for forest fire detection usingHimawari-8 satellitedata.*RemoteSens.***2018**,*10*,1992.[CrossRef]

108. Filizzola,C.;Corrado,R.;Marchese,F.;Mazzeo,G.;Paciello,R.; Pergola,N.; Tramutoli,V.RST -FIRES,an exportable algorithm for early-fire detection and monitoring: Description, implementation, and fieldvalidationinthecaseoftheMSG-SEVIRIsensor.*RemoteSens.Environ.***2017**,*192*,e2–e25.[CrossRef]

109. Di Biase, V.; Laneve, G. Geostationary sensor based forest fire detection and monitoring:An improvedversionoftheSFIDEalgorithm.*RemoteSens.***2018**,*10*,741.[CrossRef]

110. Laneve, G.; Castronuovo, M.M.; Cadau, E.G. Continuous monitoring of forest fires in the Mediterranean areausingMSG.*IEEE Trans.Geosci.Remote Sens.***2006**,*44*,2761–2768.[CrossRef]

111. Hall, J.V.; Zhang, R.; Schroeder, W.; Huang, C.; Giglio, L. Validation of GOES-16 ABI and MSG SEVIRI activefireproducts.*Int.J.Appl.EarthObs.Geoinf.***2019**, *83*, 101928.[CrossRef]

112. Schroeder, W.; Oliva, P.; Giglio, L.; Quayle, B.; Lorenz, E.; Morelli, F. Active fire detection using Landsat-8/OLIdata.*RemoteSens.Environ.***2016**, *185*,210–220.[CrossRef]

113. Larsen,A.;Hanigan,I.;Reich,B.J.;Qin,Y.;Cope,M.;Morgan,G.;Rappold,A.G.Adeeplearningapproachtoidentifysmokepl umesinsatelliteimageryinnear-realtimeforhealthriskcommunication.*J.Expo.Sci.Environ.Epidemiol.***2020**,1–7.[CrossRef]

114. Phan, T.C.; Nguyen, T.T. Remote Sensing Meets Deep Learning: Exploiting Spatio-Temporal-Spectral SatelliteImages for Early Wildfire Detection. No. REP_WORK. 2019. Available online: https://infoscience.epfl.ch/record/270339 (accessedon 7September 2020).

115. Cal Poly, S.L.O. The CubeSat Program, CubeSat Design Specification Rev.13.2014.Available online:http://blogs.esa.int/philab/files/2019/11/RD-02_CubeSat_Design_Specification_Rev._13_The.pdf(accessed on7September2020).

116. Barschke, M.F.; Bartholomäus, J.; Gordon, K.; Lehmenn, M.; Brie, K. The TUBIN nanosatellite mission forwildfiredetectioninthermalinfrared.*CEASSpace***2017**,*9*,183–194.[CrossRef]

117. Kameche, M.; Benzeniar, H.; Benbouzid, A.B.; Amri, R.; Bouanani, N. Disaster monitoring constellationusingnanosatellites.*J.Aerosp.Technol.Manag.***2014**,*6*,93–100.[CrossRef]

118. MODIS—ModerateResolutionImagingSpectroradiometer,Specifications.Availableonline:https://modis.gsfc.nasa.gov/about/specifications.php(accessed on 15 September 2020).

119. Himawari-8and9,Specifications.Availableonline:https://earth.esa.int/web/eoportal/satellite-missions/h/himawari-8-9(accessedon15September2020).

120. The SEVIRI Instrument. Available online: https://www.eumetsat.int/website/wcm/idc/groups/ops/documents/document/mday/mde1/~{}edisp/pdf_ten_msg_ seviri_instrument.pdf(accessedon15September2020).

121. GOES-16ABI,Specifications.Availableonline:https://www.goes-r.gov/spacesegment/abi.html(accessedon15September2020).

122. HuanJing-1: EnvironmentalProtection&DisasterMonitoringConstellation. Availableonline: https://earth.esa.int/web/eoportal/satellite-missions/h/hj-1(accessedon15September2020).

123. POES Series, Specifications.Available online:https://directory.eoportal.org/web/eoportal/satellite-missions/n/noaa-poes-series-5th-generation(accessedon15September2020).

124. VIIRS-375m.Available online:https://earthdata.nasa.gov/earth-observation-data/near-real-time/firms/viirs-i-band-active-fire-data(accessedon15September2020).

125. VisibleInfraredImagingRadiometerSuite(VIIRS)375mActiveFireDetectionandCharacterizationAlgorithmTheoretical Basis Document 1.0.Available online:https://viirsland.gsfc.nasa.gov/PDF/VIIRS_activefire_375m_ATBD.pdf(accessedon15September2020).

126. Shah,S.B.;Grübler,T.;Krempel,L.;Ernst,S.;Mauracher,F.;Contractor,S.Real-timewildfiredetectionfromspace—A trade-off between sensor quality, physical limitations and payload size. *Int. Arch. Photogramm.RemoteSens.Spat.Inf.Sci.***2019**.[CrossRef]

127. WebofScience.Availableonline:http://apps.webofknowledge.com/(accessedon1November2020).